BUILDING EFFECTS ON NATIONAL TRANSONIC FACILITY EXHAUST PLUME

by

K. M. Kothari*
R. N. Meroney**

Prepared for

National Aeronautics and Space Administration
Langley Research Center
Hampton, VA 23665

Fluid Mechanics and Wind Engineering Program
Department of Civil Engineering
College of Engineering
Colorado State University
Fort Collins, Colorado 80523

*Research Associate
**Professor, Civil Engineering Department

December 1979

CER79-80KMK-RNM35

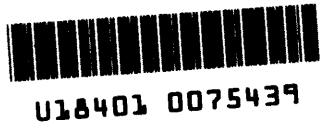

EXECUTIVE SUMMARY

As part of a program to evaluate the hazards associated with release of cold nitrogen-air mixtures from the National Transonic Facility exhaust stack, wind tunnel model tests were performed at Colorado State University to simulate the plume trajections of dense plumes as modified by the surrounding building complexes.

Photographs of plume behavior over a 1:200 scale model of the NTF complex area were examined for a range of exhaust velocities, mean wind speeds, and wind approach angle. Ground level concentrations were measured for a limited set of worst case situations. Model results suggest that the high stack exhaust velocities left the plume above most building wake structure unless wind speeds exceed 5 m/sec. Building aerodynamics appears to play a minimal role in plume fall, resulting in only a minor additional rate of drop toward the ground.

ACKNOWLEDGEMENTS

The authors wish to acknowledge the fiscal support of the National Aeronautics and Space Administration, Langley Research Center, Hampton, Virginia. The successful completion of this work depended on the encouragement of Mr. W. S. Lassiter, NASA, Langley.

TABLE OF CONTENTS

Chapter		Page
	EXECUTIVE SUMMARY	ii
	ACKNOWLEDGMENTS	iii
	LIST OF SYMBOLS	v
	LIST OF TABLES	vii
	LIST OF FIGURES	viii
1.0	INTRODUCTION	1
2.0	SIMULATION CRITERIA	1
	2.1 Simulation of Atmospheric Motion	2
	2.2 Simulation of Plume Trajectory and Dispersion	3
3.0	EXPERIMENTAL PROGRAM	5
	3.1 Wind Tunnel	5
	3.2 Model	6
	3.3 Velocity Measurements	6
	3.4 Gas Mixtures	8
	3.5 Flow Visualization Techniques	8
	3.6 Concentration Measurements	9
	3.6.1 Sample Collection System	9
	3.6.2 Sample Analysis System	9
	3.7 Data Analysis: Concentration Measurements	10
	3.8 Data Analysis: Plume Envelopes	10
4.0	TEST PROGRAM RESULTS	11
	4.1 Characteristics of the Approach Velocities	12
	4.2 Comparison of Various Scaling Criteria	12
	4.3 Influence of Building Aerodynamics on NTF Exhaust Plumes	13
5.0	CONCLUSIONS	15
	REFERENCES	16
	TABLES	17
	FIGURES	22

LIST OF SYMBOLS

Dimensions are given in terms of mass (m), length (L), time (t), and temperature (T).

Symbol	Definition	Dimensions
A, B, n	Constants in King's Law Equation	[--]
D	Diameter of Stack	[L]
E, E_{rms}	Voltage levels	[--]
Fr	Froude number	[-]
g	Gravitational constant	$[Lt^{-2}]$
H	NTF stack height	[L]
K_c	Dimensionless concentration coefficient	[-]
Q	Source strength	$[L^3t^{-1}]$
Re	Reynolds number	[-]
U, U_{rms}	Wind speed	$[Lt^{-1}]$
W_s	Stack exit velocity	$[Lt^{-1}]$
x	Along wind coordinate	[L]
$\bar{x}$	Downwind distance to maximum plume rise	[L]
x_{TD}	Touchdown distance of plume center	[L]
y_s	Distance from stack to wind-tunnel wall	[L]
y_c	Distance from camera to stack	[L]
z	Height of plume envelope from ground	[L]
z_p	Height of plume envelope from ground including parallex	[L]
z_c	Height of camera iris from model ground	[L]
χ	Concentration (ppm)	[-]
ν	Kinematic viscosity	$[L^2t^{-1}]$

Symbol	Definition	Dimensions
ρ_a	Ambient air density	$[mL^{-3}]$
ρ_s	Stack gas density	$[mL^{-3}]$
$\Delta\rho$	Density difference between source gas and ambient air	$[mL^{-3}]$
θ	Orientation angle	[-]
Δh	Plume rise	[L]

LIST OF TABLES

Table	Title	Page
1	Summary of Exhaust Plume Conditions	17
2	Summary of Tests Performed	18
3	Approach Flow Boundary Layer Characteristics	19
4	Camera and Stack Locations for Each Visualization Run	20
5	Comparison of Plume Characteristics with that Predicted by Hoot and Meroney (1974)	21

LIST OF FIGURES

Figure	Title	Page
1	Industrial Wind Tunnel Schematic	22
2	NTF Model Installed in Wind Tunnel	23
3	Parallax Correction Technique	24
4a	Velocity Profiles	25
4b	Velocity Profiles	26
5	Local Longitudinal Turbulent Intensity Profiles	27
6	NTF Exhaust Plume Envelopes, θ = 0°, U = 4 mph, W_s = 75 ft/sec, S.G. = 1.2, 1.0 and 2.0	28
7a	NTF Exhaust Plume Envelopes, θ = 0°, U = 6 mph, W_s = 75 ft/sec, S.G. = 1.2, 1.0 and 2.0	29
7b	NTF Exhaust Plume Photographs, θ = 0°, U = 6 mph, W_s = 75 ft/sec, S.G. = 1.2, 1.0 and 2.0	30
8	NTF Exhaust Plume Envelopes, θ = 0°, U = 4 mph, W_s = 150 ft/sec, S.G. = 1.2, 1.0 and 2.0	31
9a	NTF Exhaust Plume Envelopes, θ = 0°, U = 6 mph, W_s = 150 ft/sec, S.G. = 1.2, 1.0 and 2.0	32
9b	NTF Exhaust Plume Photographs, θ = 0°, U = 6 mph, W_s = 150 ft/sec, S.G. = 1.2, 1.0 and 2.0	33
10a	NTF Exhaust Plume Envelopes, θ = 0 to 225°, U = 6 mph, W_s = 150 ft/sec, S.G. = 2.0	34
10b	NTF Exhaust Plume Photographs, θ = 0 to 225°, U = 6 mph, W_s = 150 ft/sec, S.G. = 2.0	35
10c	NTF Exhaust Plume Photographs, θ = 0 to 225°, U = 6 mph, W_s = 150 ft/sec, S.G. = 2.0	36
11a	NTF Exhaust Plume Envelopes, θ = 0°, U = 4 mph, W_s = 75 and 150 ft/sec, S.G. = 2.0 with and without model complex	37
11b	NTF Exhaust Plume Photographs, θ = 0°, U = 4 mph, W_s = 75 and 150 ft/sec, S.G. = 2.0 with and without model complex	38

Figure	Title	Page
12a	NTF Exhaust Plume Envelopes, $\theta = 0°$, U = 4, 6 and 10 mph, W_s = 75 ft/sec, S.G. = 2.0	39
12b	NTF Exhaust Plume Photographs, $\theta = 0°$, U = 4, 6 and 10 mph, W_s = 75 ft/sec, S.G. = 2.0	40
13a	NTF Exhaust Plume Envelopes, $\theta = 0°$, U = 4, 6 and 10 mph, W_s = 150 ft/sec, S.G. = 2.0	41
13b	NTF Exhaust Plume Photographs, $\theta = 0°$, U = 4, 6 and 10 mph, W_s = 150 ft/sec, S.G. = 2.0	42
14	Ground Level Concentration Results	43

1.0 INTRODUCTION

The National Transonic Facility (NTF) being constructed at Langley Research Center, NASA, will emit large quantities of cold nitrogen-air mixtures which may produce ground fog under certain operational and meteorological conditions. The purpose of the present research was to obtain NTF plume characteristics using wind tunnel tests.

A 1:200 scale model of the NTF facility and surrounding buildings were placed in the Industrial Wind Tunnel at Colorado State University. Three separate gas densities were utilized to model the plume in the wind tunnel while smoke was produced by a titanium tetrachloride additive. Concentration measurements were performed to determine the quantitative character of the plume for a limited range of release conditions. The intent of these tests were to provide a data base that will enable the NTF management to determine the conditions under which operations should be limited.

Section 2 outlines the similarity requirements for modeling atmospheric flow in a wind tunnel. Experimental techniques are described in Section 3. The results and conclusions are given in Section 4.

2.0 SIMULATION CRITERIA

It is not the purpose of this report to present an exhaustive treatment of modeling the atmospheric surface layer; hence, only parameters are discussed that play a major role in the present study. For a more exhaustive treatment the reader is referred to the papers by Cermak (1975), Cermak et al. (1966) and Snyder (1972).

2.1 Simulation of Atmospheric Motion

Generally, the similarity requirements are: (1) undistorted scaling of boundary geometry (geometric similarity), (2) kinematic similarity of approach flow (distributions of mean velocity and turbulence characteristics), (3) Rossby number equality, (4) Reynolds number equality and (5) bulk Richardson number equality.

For the neutral flow conditions considered in the present study the bulk Richardson number equality is satisfied. For localized flow investigations where Coriolis effects are not important, as in this study, Rossby number equality can be relaxed.

The Reynolds number represents the ratio of characteristic inertial to viscous forces. Since the Reynolds number is usually lower in the wind tunnel test this implies that viscous forces in the model are more dominant than in the corresponding prototype flow. However Golden (1961) has shown that a diffusion critical Reynolds number exists. Flows with Reynolds numbers which exceed this critical number produce concentration patterns downwind of buildings which are invariant with velocity magnitude. Golden determined that this critical Reynolds number is 11,000. Fortunately, even when the Reynolds number exceeds 3500 there is little detectable variation in the far field plume behavior. The minimum and maximum Reynolds numbers during the flow visualization study were 2440 and 12600 respectively. The Reynolds number during the concentration measurement was 19300. The Reynolds number was based on the height of stack and approach flow velocity at the stack height.

2.2 Simulation of Plume Trajectory and Dispersion

Once geometric and kinematic similarity for the simulated atmospheric boundary layer are achieved, additional modeling requirements for similar plume behavior can be stipulated as follows.

1. Equality of density ratio ρ_s/ρ_a,
2. Consistent scaling of all velocities (W_s/U),
3. Equality of Froude number $(\rho_a W_s^2/(g \Delta\rho D))$,
4.* Equal momentum ratio $(\rho_s W_s^2)/(\rho_a U^2)$,
5.* Equality of $(\rho_a U^3)/(g \Delta\rho D W_s)$ and
6. Equality of stack Reynolds number DW_s/ν_s

where ρ_s and ρ_a are stack gas density and atmospheric air density respectively, W_s and U are the exhaust velocity and reference velocity in the approach flow (10 m prototype) respectively, $\Delta\rho$ is the difference between the exhaust gas density and density of atmospheric air, D is stack diameter and ν_s is the kinematic viscocity of the stack gas.

The model stack Reynolds number must be lower than the prototype stack Reynolds number; and, indeed, the low Reynolds number would imply that the flow through the stack exits in a laminar manner rather than the turbulent jet observed above the prototype vent. To assure a turbulent exhaust jet, Snyder (1972) and others suggest one add a surface trip inside the stack to obtain a fully turbulent exhaust. The diameter of the stack was tripped at a distance of 3D from the top of the stack with a 0.75D collar. This provided an exhaust jet from the model stack which exited as a fully turbulent flow.

*Equality of 1, 2, and 3; 1, 3, and 4 or 1, 2, and 5 are equivalent.

The prototype equivalent values and alternative plume rise criteria selected for different runs are given in Table 1.

Criteria one stipulates equality of density ratio, volume flux, and Froude number and assures exact model similitude. The utilization of criteria one to reproduce the behavior of dense plumes emitted from stacks and at ground level has been discussed by Hoot and Meroney (1974) and Meroney (1979). Unfortunately the small model scale requires extremely low reference wind velocities, which are less than 0.15 m/sec. At such low velocities the instrumentation becomes increasingly inaccurate; in addition, the stalling pitch required on the wind tunnel fan is difficult to set. Often the wind speed remains erratic and non-stationary. Although such conditions could be arranged for short periods with exacting attention to detail and frequent delays; it is more efficient to select alternative model criteria which permit higher tunnel speeds for the bulk of the experimental conditions.

Criteria two relaxes equality of density ratio and Froude number but stipulates equivalent momentum ratio of effluents at stack exit. In this case ambient air is used as the exhaust gas; however it is exhausted at higher velocities to assure momentum equality. No constraint exists on wind tunnel velocity other than equivalent velocity and turbulence profiles shape. The plume initial trajectory near the NTF facility will be equivalent to that of a dense plume; however, the plume will show no tendency to drop further downward. Final plume rise will be less than that of a buoyant plume or more than that of a dense plume. Utilizing an ambient gas in place of a buoyant plume has been previously proposed by Cermak and Nayak (1973). The plume envelopes provide a reference condition against which to compare the effects of negative buoyancy.

Criteria three relaxes equality of density ratio while stipulating equality of momentum ratio and buoyancy flux (i.e. equality of conditions 4 and 5 above). This partial simulation relaxes the requirement of stack density in favor of operating at higher model wind speeds. Skinner and Ludwig (1978) showed that by exaggerating the buoyancy and exit momentum of the stack effluent, and compensating with an increase in wind speed, the same dispersion is obtained as when the restriction of modeling the ratio of stack exit density to ambient density is applied. Neff and Meroney (1979) used similar criteria while modeling the behavior of liquid natural gas spills. Unfortunately, there is disagreement within the modeling community as to the efficacy of approximate modeling methods. Isyumov and Tanaka (1979) reported a comparative study of five relaxed stack gas dispersion techniques. They concluded all approximation methods exaggerate the influence of density at extended distances. For dense plumes this might suggest an exaggerated drop of the plume centerline; fortunately, this represents a conservative condition for purposes of this study.

3.0 EXPERIMENTAL PROGRAM

3.1 Wind Tunnel

All measurements were made in the Industrial Aerodynamics Wind Tunnel located in the Fluid Dynamics and Diffusion Laboratory of Colorado State University, Fort Collins, Colorado. A schematic of the wind tunnel and photograph of the interior are shown in Figure 1 and 2, respectively. This is a closed circuit wind tunnel powered by a 75 hp single speed induction motor. A 16 blade variable pitch axial fan provides control of the speed in the tunnel. The square cross section of

the tunnel is 3.3 m^2 and the length of the test section is 18.3 m. The contraction ratio at the entrance of the test section is 4:1. The selectable velocity magnitude in the test section ranges from 0.5 m/sec to 24 m/sec. The ceiling of the last 7.3 m of the test section is adjustable, allowing removal of any longitudinal pressure gradient in the wind tunnel. To maintain the lower velocity required for criteria 1 and criteria 3, cardboard plates with 3/16-inch diameter holes on 1-inch center to center were installed at the rear of the wind tunnel. The total open area ratio provided by the punched plates was 2.6%. The plate produces a large wind tunnel pressure drop reducing the wind speed in the test section area. Measurements of velocity and turbulence intensity performed at various downwind locations of the wind tunnel show no appreciable variability; and the velocity in free stream was steady.

The long test section in conjunction with spires and roughness elements (1.25 cm high) on the floor of the wind tunnel were used to generate a thick turbulent boundary layer.

3.2 Model

A 1:200 scale model of the NTF Facility and surrounding buildings was constructed from styrofoam blocks. The stack itself was formed from a brass tube. The height and diameter of the model stack were 18.3 cm (7.2 inch) and 1.6 cm (0.62 inch), respectively. The detailed model extends about 180 m (600 ft) in a circular arc having a center about 61 m (200 ft) north of the NTF stack. Figure 2 shows the model placed in the Industrial Wind Tunnel.

3.3 Velocity Measurements

Measurements of mean velocity and turbulence intensity were accomplished with a single hot-film anemometer with film axis horizontal.

The instrumentation used was a Thermo-Systems constant temperature anemometer model 1050 connected to a 2.54×10^{-3} cm diameter platinum film sensing element 0.0508 cm long. The output of the constant temperature anemometer was directed to an on-line data acquisition system consisting of a Hewlett-Packard 21 MX Computer, disc unit, card reader, printer, Digi-Data digital tape drive and a Preston Scientific Analog-digital converter. The data was processed immediately into mean velocity and turbulence intensity at each corresponding height and stored on the computer disc for printout or further analysis.

Calibration of the hot-wire anemometer was performed using a calibrator suitable for low velocity and developed by CSU staff. The calibration data were fit to a variable exponent King's law relationship

$$E^2 = A + BU^n$$

where E is the hot-wire output voltage, U is the velocity and A, B and n are coefficients selected to fit the calibration data. All measurements were performed with a sample rate of 250 samples per second for 20 seconds, and the above calibration relationship was used to determine the mean velocity. The King's Law relationship is not normally used for very low velocities where the heat transfer from the sensor is governed by mixed forced/free convection; hence, the low velocity measurements obtained by the hot-film are somewhat questionable. Absolute accuracy is probably no better than ±20% at such low velocities; however relative magnitudes are consistent. The fluctuating velocity may be characterized by the statistic U_{rms} (root-mean-square velocity). It was calculated from

$$U_{rms} = \frac{2E\ E_{rms}}{Bn\ U^{n-1}}$$

where E_{rms} is the root-mean-square of the voltage output from the anemometer. The local turbulence intensity, U_{rms}/U, was then calculated.

3.4 Gas Mixtures

In order to conduct tests with three different specific gravity gases, three different gas mixtures were used. For criteria 1, a gas mixture of 9.86% Propane (C_2H_6), 37.9% (CO_2) and 52.4% (N_2) was used to produce a gas having a net specific gravity of 1.2. For criteria 2, commercially available air was used. For criteria 3, a mixture of 32.5% Freon-12 and 67.5% air was prepared. The latter gas was mixed using a pressure ratio technique; thus only an approximate gas content was known; nonetheless, a specific gravity equal to 2 ± (.10) was obtained.

3.5 Flow Visualization Techniques

Smoke was used to visually define the plume envelope emitted from the model stack of the NTF facility. The smoke was produced by passing the mixture of the gases stored in a Matheson gas cylinder, through a Fischer & Porter flow controller into a container of titanium tetrachloride located outside the wind tunnel. Smoke produced by the interaction of titanium tetrachloride and moisture in the gas mixture was transported through the wind tunnel wall by means of a tygon tube terminating at the stack inlet. The flow rates stipulated were adjusted by the flow controller using the calibration charts furnished by Fischer & Porter accounting for the change in molecular weight and barometric pressure.

The plume was illuminated with carbon arc-lamp beams. A visible record was obtained by means of black and white pictures taken with a 35 mm Speed Graphic camera color slides and 16 mm silent movie film taken with a Bolex motion picture camera. The plume spread was determined from black and white still pictures each exposed from 1/20 to 1/30 sec.

3.6 Concentration Measurements

Two sets of concentration data were obtained. One set consists of concentration measurements in the absence of the NTF facility and surrounding building complexes, but from an equivalent isolated NTF stack; whereas the second set was with the NTF facility and buildings present. For each data set measurements were performed at three locations along the centerline of stack plus a background sample. When the NTF facility was present, the test was performed for a wind direction of 180°. During the concentration measurements, the gas mixture for criteria 1 was utilized.

Once the release of the tracer gas began, the sample collection system was flushed several times; subsequently a sample was drawn over a period of approximately 60 seconds and held for subsequent analysis. Once samples were isolated the tracer gas flows were immediately terminated to prevent background build up in the wind tunnel.

3.6.1 Sample Collection System

Four 3.2 mm tygon sample tubes approximately 8 m in length were fed through the wind-tunnel wall, and each was fastened at a sample grid location. The tubes led to a sample withdrawal and containment system designed and built by the CSU staff. Each sample was held secure in 30 cc plexiglass syringes by isolating valves. The sample was expelled from the syringes to the analyzer.

3.6.2 Sample Analysis System

A Hewlett-Packard 5700A gas chromatograph with a flame ionization detector (FID) was used to analyze the sample. The oven was maintained at 145°C and the detector at 250°C with a carrier flow rate through the column of approximately 55 cc/min. The column was a 3.2 mm x 2m long Purepak-R column and the carrier gas was nitrogen.

The principle of operation of a chromatograph requires that the compounds be separated by molecular size as they pass through an absorbing column. As each hydrocarbon compound elutes from the column into the FID it is burned in a hydrogen flame and ionized. The voltage potential produced across the detector is measured by an electrometer, amplified and directed to an integrator. The gas chromatograph was calibrated prior to each day's operation by standard gas mixtures.

3.7 Data Analysis: Concentration Measurements

The concentration data were reduced to a nondimensional concentration coefficient, K_c. The coefficient K_c is defined as

$$K_c = \frac{\chi\ U\ H^2}{\chi_{source}\ Q_{source}}$$

where χ is the located concentration (ppm)

U is the reference velocity at release height (m/sec)

H is the reference height (height of stack), (m)

χ_{source} is the source strength (ppm)

Q_{source} is the source flow rate (m^3/sec).

3.8 Data Analysis: Plume Envelopes

Smoke emitted with the respective exhaust plumes were photographed against a square grid matrix located on the back wind tunnel wall. Position of the cameras with respect to the wind tunnel and the exhaust stack were recorded during each experiment. Knowledge of the relative locations of camera, stack, and background grid permitted one to correct plume envelopes recorded by the photographs for parallax.

Each photograph was individually examined and the outline envelope of maximum vertical dispersion identified. The x-y location of the plume envelope was digitized using a auto-trol coordinatograph digitizer

which also produced accompanying sets of punched computer cards. Plume envelope heights from ground level were connected by the following formula:

$$z = z_p - (z_p - z_c)\left(\frac{y_s}{y_s + y_c}\right)$$

where z = actual plume envelope height

z_p = plume envelope height including parallel

z_c = height of camera iris from model gravel

y_s = distance from model stack to background wind tunnel wall

y_c = distance from camera to model stack.

The sketch in Figure 3 identifies relative location of all dimensions. Figures 6 to 13 represent plume envelopes corrected for parallax in the manner outlined above.

4.0 TEST PROGRAM RESULTS

The test program consisted of two test series with and without building complex present, and three exhaust plume densities, specific gravities of 1.2, 1.0 and 2.0. The test series objectives were:

- To verify that approximate scaling criteria three is equivalent to, or at least more conservative than, exact similitude criteria one.
- To estimate plume trajectories and plume envelopes over a range of exhaust velocity and wind speed conditions.
- To examine the influence of building complex aerodynamics on the loft of NTF exhaust plumes for various wind approach directions.

A summary of all tests simulated in the laboratory is presented in Table 2. Only a few visualization photographs are reproduced in this report. A complete set of black and white photographs, color slides, and an annotated 16 mm film have been provided under separate cover to

the contractor at NASA, Langley. All dimensions reported in the following sections have been converted to equivalent field full-scale values appropriate to the NTF site. Origin in plume envelope figures is referenced to the left of the NTF exhaust stack at ground. The position x-axis is in the direction of prevailing wind for all coordinate systems.

4.1 Characteristics of the Approach Velocities

Measurements of the approach flow characteristics were obtained for the modeled flow over the NTF scaled complex. As discussed in Section 3.1 to 3.3 these characteristic profiles should be comparable to those expected over the NTF complex site. Counihan (1975) has summarized the values of aerodynamic roughness, z_o, and power law index, p, that may be expected to occur in the atmosphere. Table 3 summarizes approach wind field characteristics measured. Figures 4 and 5 display pertinent velocity profiles and longitudinal turbulent intensity profiles. As expected the lower wind speeds characteristic to model criteria one were difficult to maintain stationary; in addition the low Reynolds' numbers associated with these flows seemed to result in slightly larger values of power-law index p characteristic of relaminarizaton of the turbulence.

4.2 Comparison of Various Scaling Criteria

As discussed at length in Section 2.2 constraints on wind tunnel operations require the use of relaxed or approximate simulation criteria to specify model exhaust characteristics. A series of measurements were performed to evaluate the perturbations introduced by such approximations.

As expected over the momentum dominated portion of plume rise model criterias one, two, and three produce essentially equivalent plume envelope outlines. The momentum dominated trajectory appears to extend

20 meters downwind for all cases examined. Downwind of this point buoyancy forces dominate plume trajectory and the denser plumes drop. Examination of Figures 6 through 9 suggests that Model Criteria three systematically results in lower plumes than Model Criteria one; nonetheless the differences are small for the lower envelope outline. Only small errors should result from the use of the conservative model criteria three plumes.

It is suspected that the differences between plume envelopes for criteria one versus three have been exaggerated by a systematic tendency to set wind velocities at too low a value for criteria one situations. This error was only discovered after all measurements were completed. Setting the reference wind velocity low by up to 25% for criteria one situations would results in plumes which loft higher than the equivalent criteria three cases. On the other hand the results of Isyumov and Tanaka (1979) suggest criteria three exaggerates plume rise for buoyant plumes, which would translate into exaggerated plume fall for dense plumes. It is not possible to conclude decisively that full similitude has been obtained based on the present measurements; nonetheless, errors should be reasonably small and conservative.

4.3 Influence of Building Aerodynamics on NTF Exhaust Plumes

The turbulence excess produced by wakes of the building complex appeared to influence the NTF exhaust plume to the same extent for all wind directions examined. The results on Figure 10 suggest that only minor variations occur for different wind directions; however an orientation of $\theta = 0$ degrees might be considered slightly more critical. Subsequent comparisons will be limited to intercomparisons made for an orientation of zero degrees.

The excess turbulence created by building interaction with the approach boundary layer definitely accelerates downward transport of the lower plume boundary. In Figure 11 plumes in the presence and absence of the model buildings are compared for equivalent velocity conditions. It would appear that building wake interaction draws the plume to the surface some forty to fifty meters nearer the stack then gases released from an isolated stack. Nonetheless, in terms of total transport distances and expected variations among individual realizations of the plume trajectory, this is a relatively small correction.

Only the upper plume envelope is affected significantly by increasing wind speed as shown in Figures 12 and 13 for exhaust stack velocities of 75 and 150 ft/sec respectively. These curves reflect the respective changes in wind versus exhaust jet momentum as the wind speed changes. For a given exhaust velocity the lower plume boundary seems to descend at nearly constant rate independent of wind speed. This suggests that once the lower plume boundary crosses the building wake region the vertical transport by turbulent diffusion exceeds the falling trajectory effect of the dense gas. Since the building wake kinematics should be independent of Reynolds number, an increase in wind speed should have no strong effect.

In any event, for wind speeds less than 10 mph and stack exhaust velocities greater than 75 ft/sec, no lower plume envelope reaches the ground before 160 meters downwind of the NTF stack. For stack exhaust velocities of 150 ft/sec the lower plume envelope intersects the ground at distances exceeding 200 meters.

Ground surface level concentration measurements were only made for a limited set of situations. A wind orientation of $\theta = 180°$ was chosen

for these measurements. Figure 14 compares the nondimensional concentration coefficient values measured at various downwind distances against values measured in the absence of the building complex.

The present results of the concentration measurements, plume rise, Δh, downwind distance to maximum plume rise, $\bar{x}$ and touchdown distance of plume center, x_{TD} are compared against the prediction by Hoot and Meroney and presented in Table 5. On an average the results show good comparison except for the case of 4 mph wind and exhaust velocity of 75 ft/sec.

5.0 CONCLUSIONS

Exhaust plume visualization and concentration measurements of a 1:200 scale model of the NTF Vent Stack and surrounding buildings in the CSU Industrial Aerodynamics Wind Tunnel have resulted in the following conclusions:

- Building effects could draw the NTF plume to the ground 40-50 m nearer the vent stack. However, the distance from the vent stack to plume touchdown is always greater than 160 m, for wind speeds from 4-10 mph.
- Wind direction has little effect on the building wake interference of the NTF plume.
- Only the upper plume boundary appears affected by the wind speed. The lower boundary appears to descend at a rate independent of wind speed, suggesting that vertical diffusion in the building wake exceeds negative buoyant effects.
- The momentum dominated trajectory of the NTF plume extends at least 20 m downwind, beyond which buoyancy forces dominate and denser plumes descend.

REFERENCES

Cermak, J. E., Sandborn, V. A., Plate, E. J., Binder, G. H., Chuang, H., Meroney, R. N., and Ito, S. (1966). "Simulation of Atmospheric Motion by Wind-Tunnel Flows," Colorado State University, Civil Engineering Report CER66-17, 101 p.

Cermak, J. E. (1975). "Applications of Fluid Mechanics to Wind Engineering--A Freeman Scholar Lecture," Jour. of Fluids Engineering, ASME, Vol. 97, Series 1, No. 1, March 1975.

Cermak, J. E. and Nayak, S. K. (1973). "Wind-Tunnel Model Study of Downwash from Stacks at Maui Electric Company Power Plant, Kahului, Hawaii," Colorado State University, Civil Engineering Report CER72-73JEC-SKN28, 58 p.

Counihan, J. (1975). "Adiabatic Atmosphere Boundary Layers: A Review and Analysis of Data from the Period 1880-1972," Atmospheric Environment, Vol. 9, pp. 871-905.

Hoot, T. and Meroney, R. N. (1974). "The Behavior of Negatively Buoyant Stack Gases," 67th APCA Proceedings, Denver, Colorado, 20 p.

Isyumov, N. and Tanaka, H. (1979). "Wind Tunnel Modeling of Stack Gas Dispersion - Difficulties and Approximations," Proceedings of the 5th International Wind Engineering Conference, Fort Collins, Colorado, July 1979, 26 p.

Meroney, R. N. (1979). "Physical Modeling of Atmospheric Dispersion of Heavy Gases Released at the Ground as from Short Stacks," Proceedings of 10th International Technical Meeting on Air Pollution Modeling and Its Application, 23-26 October 1979, Rome, Italy, 9 p.

Neff, D. E. and Meroney, R. N. (1979), "Dispersion of Vapor from LNG Spills--Simulation in a Meteorological Wind Tunnel of Spills at China Lake Naval Weapons Center, California," Colorado State University, Civil Engineering Report CER78-79DEN-RNM41, 77 p.

Skinner, G. T. and Ludwig, G. R. (1978), "Physical Modeling of Dispersion in the Atmospheric Boundary Layer," CALSPAN Report No. 201, New York, 31 p.

Snyder, W. H. (1972), "Similarity Criteria for the Application of Fluid Models to the Study of Air Pollution Meteorology," Boundary Layer Meteorology, Vol. 3, pp. 113-134.

Table 1. Summary of Exhaust Plume Conditions

No Building Reference Conditions: (Equivalent prototype values)

Wind Direction	Prototype Plume Density	Modeled Plume Density	Prototype Exhaust Velocities	Prototype Wind Speeds	Visualization Test Cases
1	1.2	1.2*	75 (ft/sec)	4 mph	4
			150	6	
1	1.2	1.0$^{\Delta}$	75	4	4
			150	6	
1	1.2	2.0$^{\nabla}$	75	4	12
			150	6	
			200	8	
				10	

NTF Model Release Conditions

Wind Direction	Prototype Plume Density	Modeled Plume Density	Prototype Exhaust Velocities	Prototype Wind Speeds	Visualization Test Cases
1	1.2	1.2*	75	4	4
			150	6	
1	1.2	1.0$^{\Delta}$	75	4	
			150	6	
8	1.2	2.0$^{\nabla}$	75	4	96
			150	6	
			200	8	
				10	

*Model Criteria 1: $[\rho_s/\rho_a]$, $[W_s/U]$, $[\rho_a W_s^2/g\Delta\rho D]$

ΔModel Criteria 2: $[\rho_s W_s^2/\rho_a U^2]$

∇Model Criteria 3: $[\rho_s W_s^2/\rho_a U^2]$, $[\rho_a U^3/g\Delta\rho D W_s]$

Table 2. Summary of Tests Performed

Run # with NTF Complex	Criteria	$(W_s)_p$ ft/sec	$(W_s)_p$ m/sec	$(W_s)_m$ m/sec	$(U)_p$ mph @10 m Height	$(U)_p$ m/sec @10 m Height	$(U)_m$ m/sec @5 cm Height	$(U)_m$ m/sec @115 cm Height	Run # without NTF Complex
1	1	75	22.85	1.62	4	1.78	0.13	0.24	21
2	1	150	45.69	3.23	4	1.78	0.13	0.24	22
3	1	75	22.85	1.62	6	2.68	0.19	0.36	23
4	1	150	45.69	3.23	6	2.68	0.19	0.36	24
41	2	75	22.85	14.69	4	1.78	1.05	2.0	45
42	2	150	45.69	29.38	4	1.78	1.05	2.0	46
43	2	75	22.85	9.75	6	2.68	1.05	2.0	47
44	2	150	45.69	19.51	6	2.68	1.05	2.0	48
9	3	75	22.85	2.45	4	1.78	0.25	0.47	29
10	3	150	45.69	4.91	4	1.78	0.25	0.47	30
11	3	200	60.92	6.55	4	1.78	0.25	0.47	31
12	3	75	22.85	2.45	6	2.68	0.37	0.70	32
13	3	150	45.69	4.91	6	2.68	0.37	0.70	33
14	3	200	60.92	6.55	6	2.68	0.37	0.70	34
15	3	75	22.85	2.45	8	3.57	0.49	0.93	35
16	3	150	45.69	4.91	8	3.57	0.49	0.93	36
17	3	200	60.92	6.55	8	3.57	0.49	0.93	37
18	3	75	22.85	2.45	10	4.47	0.62	1.18	38
19	3	150	45.69	4.91	10	4.47	0.62	1.18	39
20	3	200	60.92	6.55	10	4.47	0.62	1.18	40

Wind directions for Run #'s 9 to 20 are indicated on photographs by letters A through H corresponding to 0° to 315° in increments of 45°.

Table 3. Approach Flow Boundary Layer Characteristics

Criteria	$(U)_p$ mph	$\frac{u_*}{U(H)}$	$\frac{z_o}{H}$	n
1	4	4.75×10^{-3}	0.018	0.26
1	6	4.75×10^{-3}	0.018	0.26
3	4	4.65×10^{-3}	0.018	0.25
3	6	5.10×10^{-3}	0.018	0.23
3	8	4.70×10^{-3}	0.018	0.19
3	10	4.75×10^{-3}	0.018	0.18
2	4 or 6	4.70×10^{-3}	0.018	0.18
	Average	4.77×10^{-3}	0.018	0.22

Table 4. Camera and Stack Locations for Each Visualization Run

Run #	y_c Meters			y_s Meters			z_c Meters		
	Movie	4 x 5	Slide	Movie	4 x 5	Slide	Movie	4 x 5	Slide
1 to 4	1.98	2.06	2.00	0.91	0.91	0.91	0.28	0.32	0.29
9 to 14 A	1.98	2.06	2.00	0.91	0.91	0.91	0.28	0.32	0.29
9 to 14 B	2.20	2.27	2.22	0.70	0.70	0.70	0.28	0.32	0.29
9 to 14 C	2.28	2.36	2.31	0.61	0.61	0.61	0.28	0.32	0.29
9 to 14 D	2.20	2.27	2.22	0.70	0.70	0.70	0.28	0.32	0.29
9 to 14 E	1.98	2.06	2.00	0.91	0.91	0.91	0.28	0.32	0.29
9 to 14 F	1.76	1.84	1.79	1.13	1.13	1.13	0.28	0.32	0.29
9 to 14 G	1.67	1.75	1.70	1.22	1.22	1.22	0.28	0.32	0.29
9 to 14 H	1.76	1.84	1.79	1.13	1.13	1.13	0.28	0.32	0.29
15 to 20 A	2.60	2.33	2.52	0.91	0.91	0.91	0.35	0.35	0.34
15 to 20 B	2.81	2.74	2.54	0.70	0.70	0.70	0.35	0.35	0.34
15 to 20 C	2.90	2.63	2.82	0.61	0.61	0.61	0.35	0.35	0.34
15 to 20 D	2.81	2.74	2.54	0.70	0.70	0.70	0.35	0.35	0.34
15 to 20 E	2.60	2.33	2.52	0.91	0.91	0.91	0.35	0.35	0.34
15 to 20 F	2.38	2.11	2.30	1.13	1.13	1.13	0.35	0.35	0.34
15 to 20 G	2.29	2.02	2.21	1.22	1.22	1.22	0.35	0.35	0.34
15 to 20 H	2.38	2.11	2.30	1.13	1.13	1.13	0.35	0.35	0.34
21 to 24 and 29 to 48	2.60	2.33	2.52	0.91	0.91	0.91	0.35	0.35	0.34

Lens Specification

movie 16-100 mm zoom
4 x 5 127 mm
slide 35 mmx 70 mm zoom

Table 5. Comparison of Plume Characteristics with that Predicted by Hoot and Meroney (1974)

$(W_S)_p$ ft/sec	$(U)_p$ mph @ 10m Height	Downwind Distance to Maximum Plume Rise, $\bar{x}$ Meters		Touchdown Distance of Plume Center, x_{TD}, Meters		Plume Rise Δh Meters		K_c(maximum)	
		Calculated	Experimental	Calculated	Experimental	Calculated	Experimental	Calculated	Experimental
75	4	32	65	156	240	45	46	0.26	--
75	6	49	45	255	250	39	41	0.32	--
75	50	--	--	--	--	--	--	0.80	0.46*
150	4	63	70	255	325	89	75	0.09	--
150	6	98	90	410	330	77	70	0.11	--

*Wind direction = 180° and maximum measured value with NTF complex
All other experimental data are for wind direction = 0°

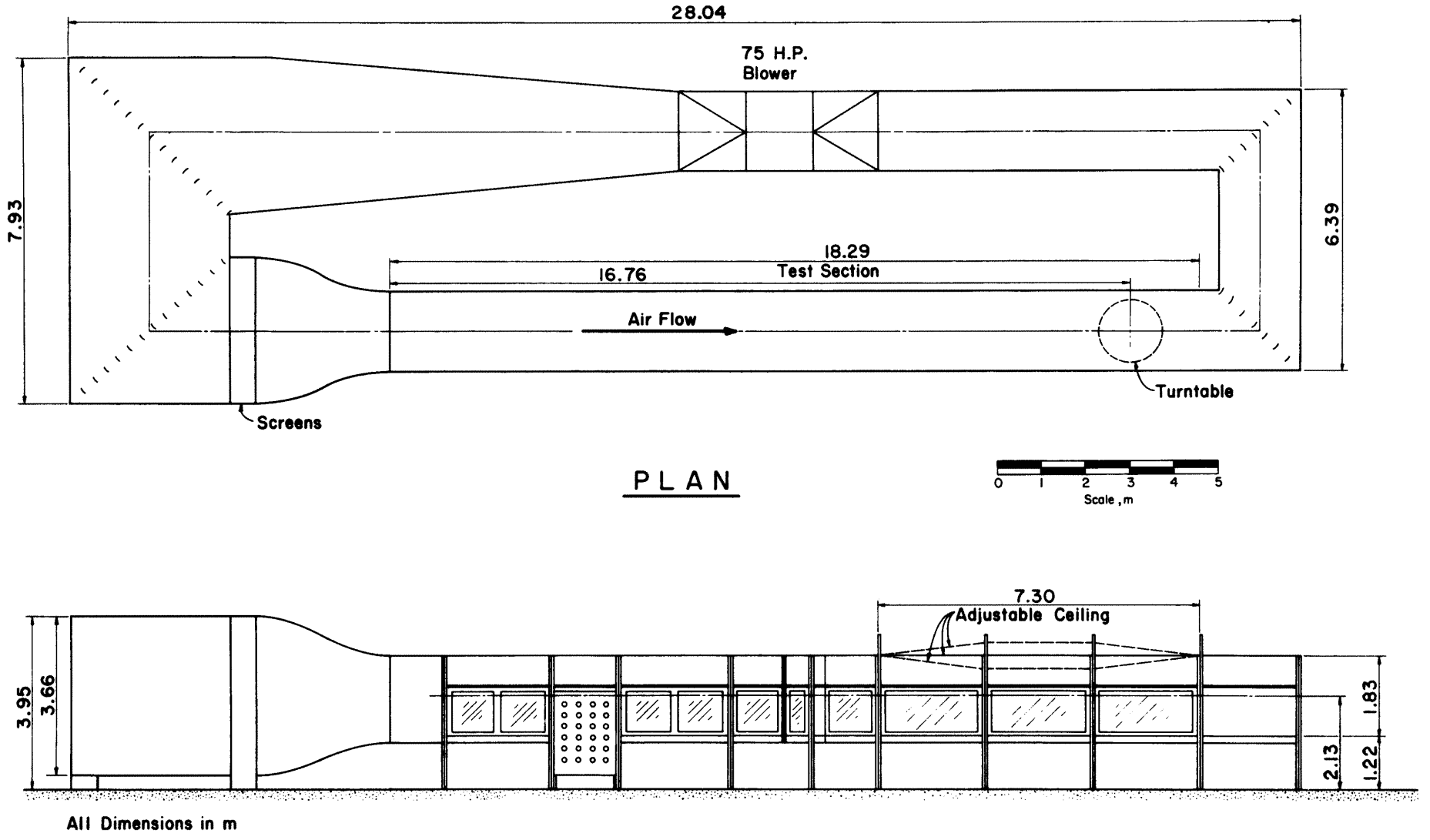

Figure 1. Industrial Wind Tunnel Schematic

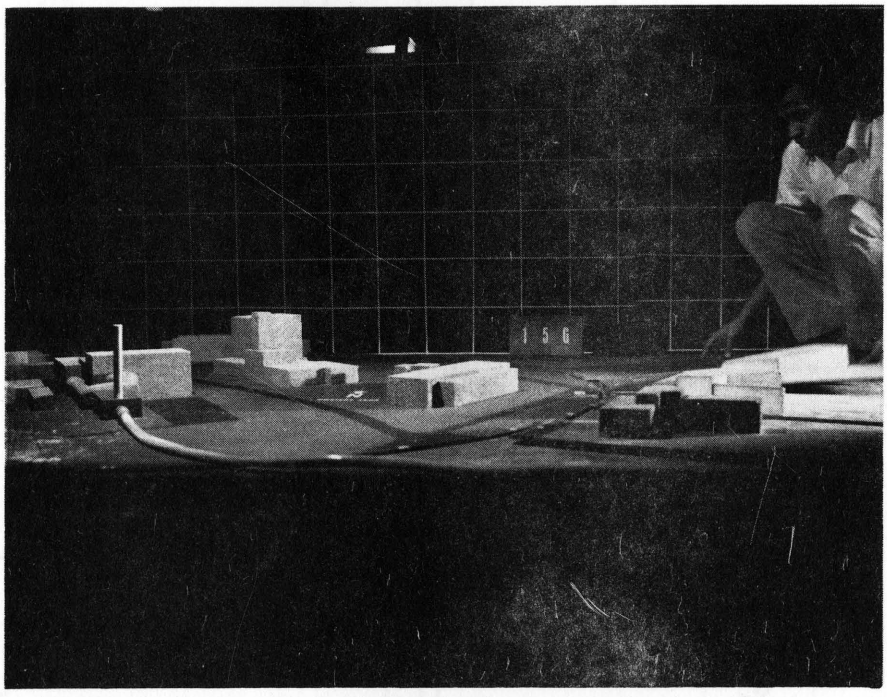

Figure 2. NTF Model Installed in Wind Tunnel

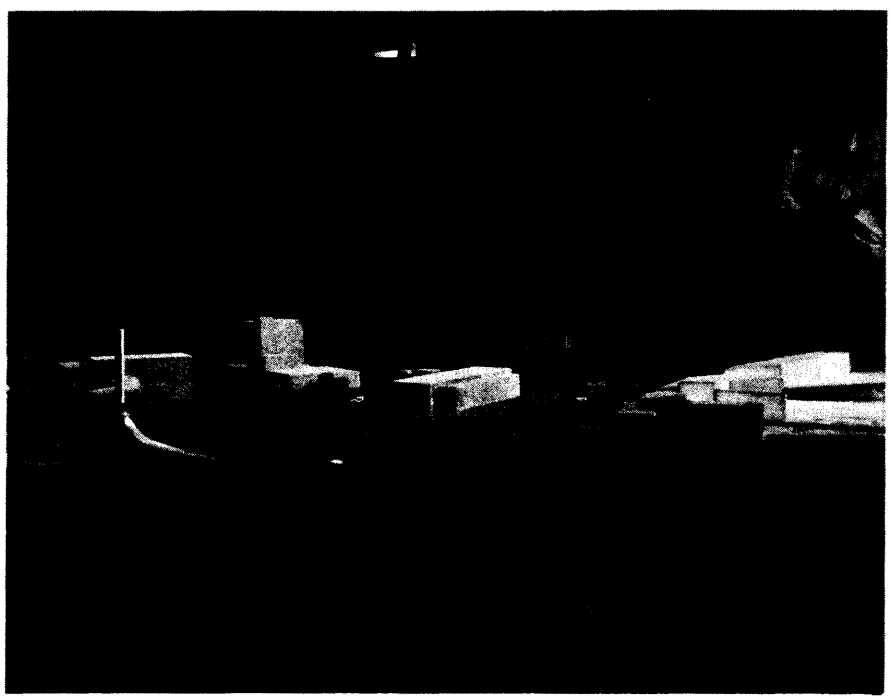

Figure 2. NTF Model Installed in Wind Tunnel

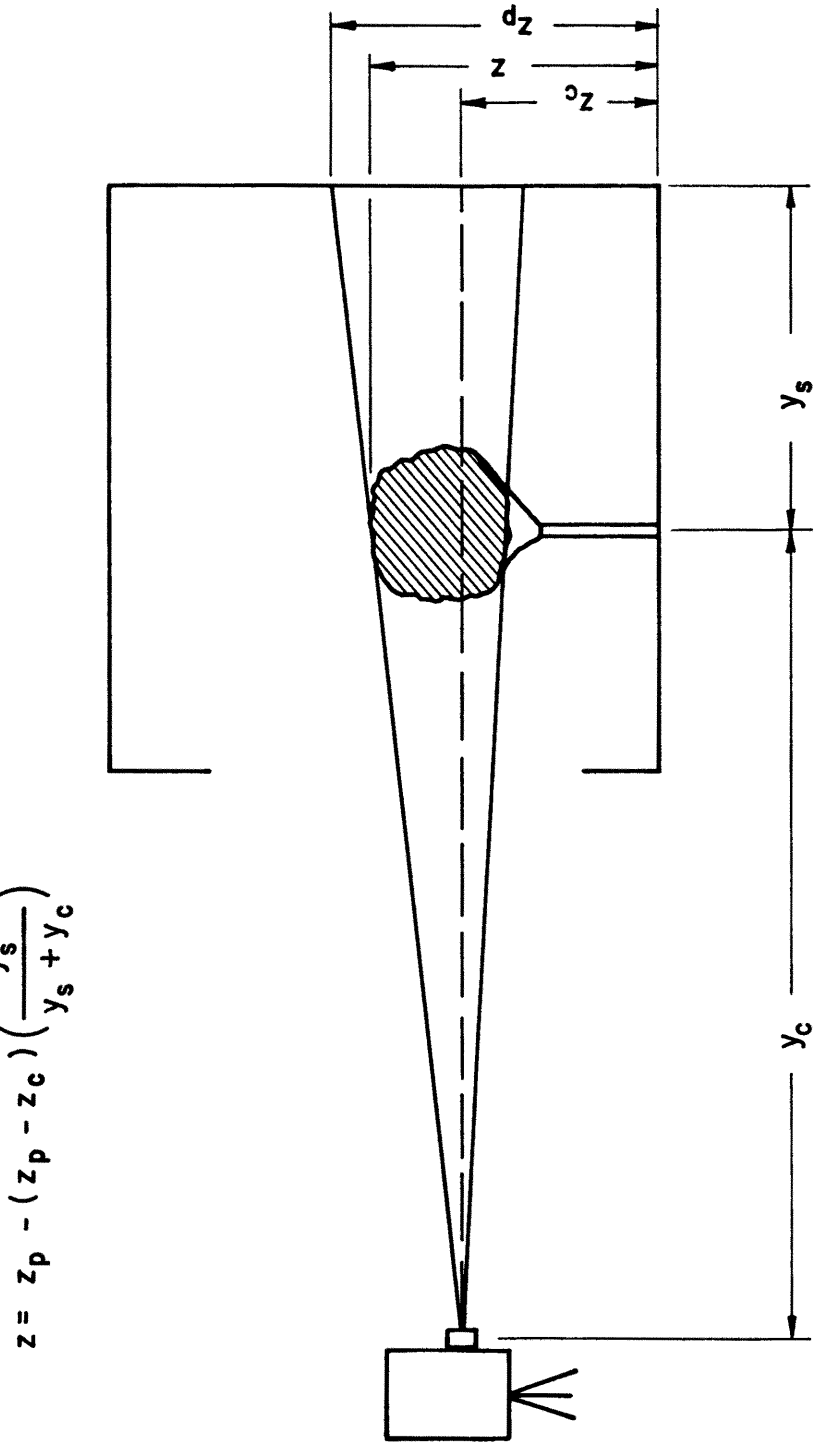

Figure 3. Parallax Correction Technique

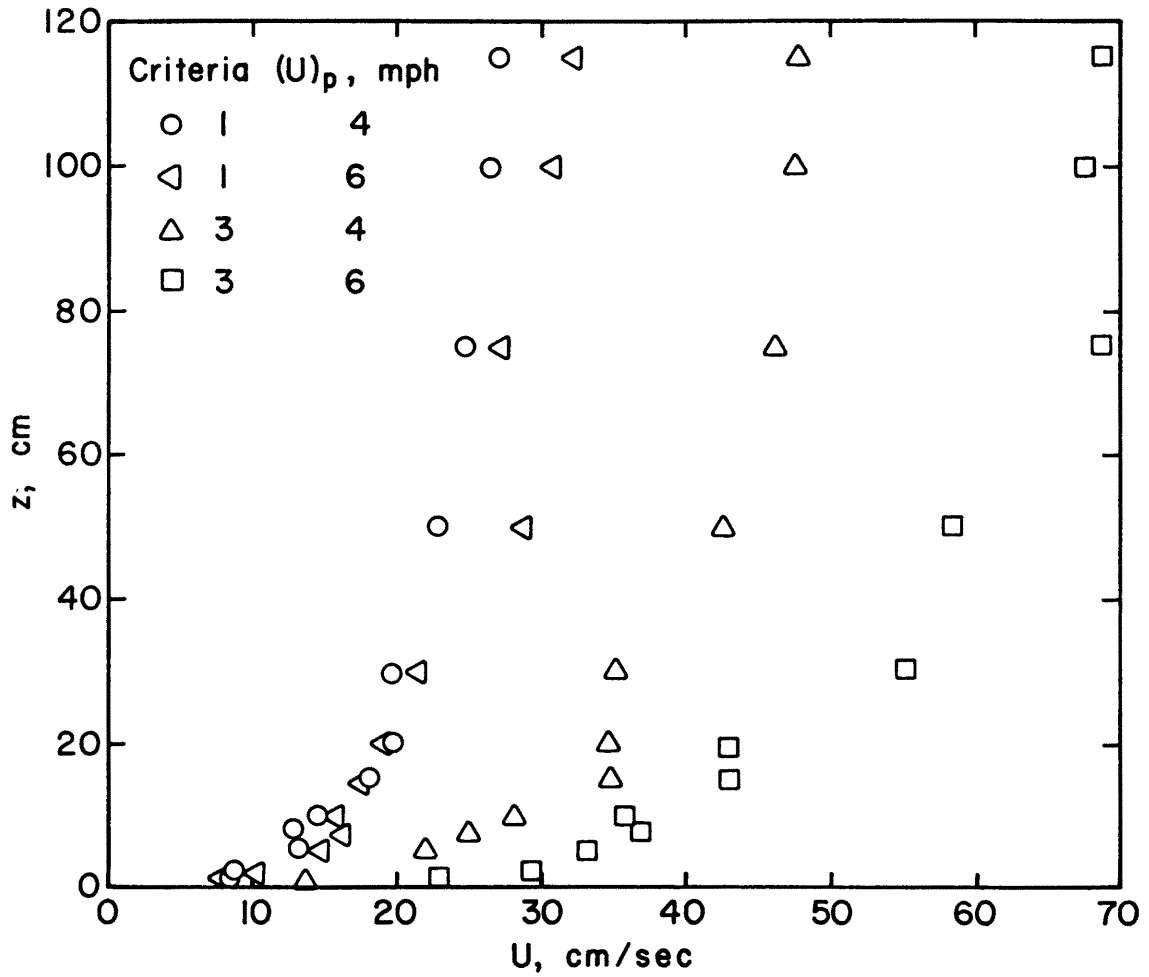

Figure 4a. Velocity Profiles

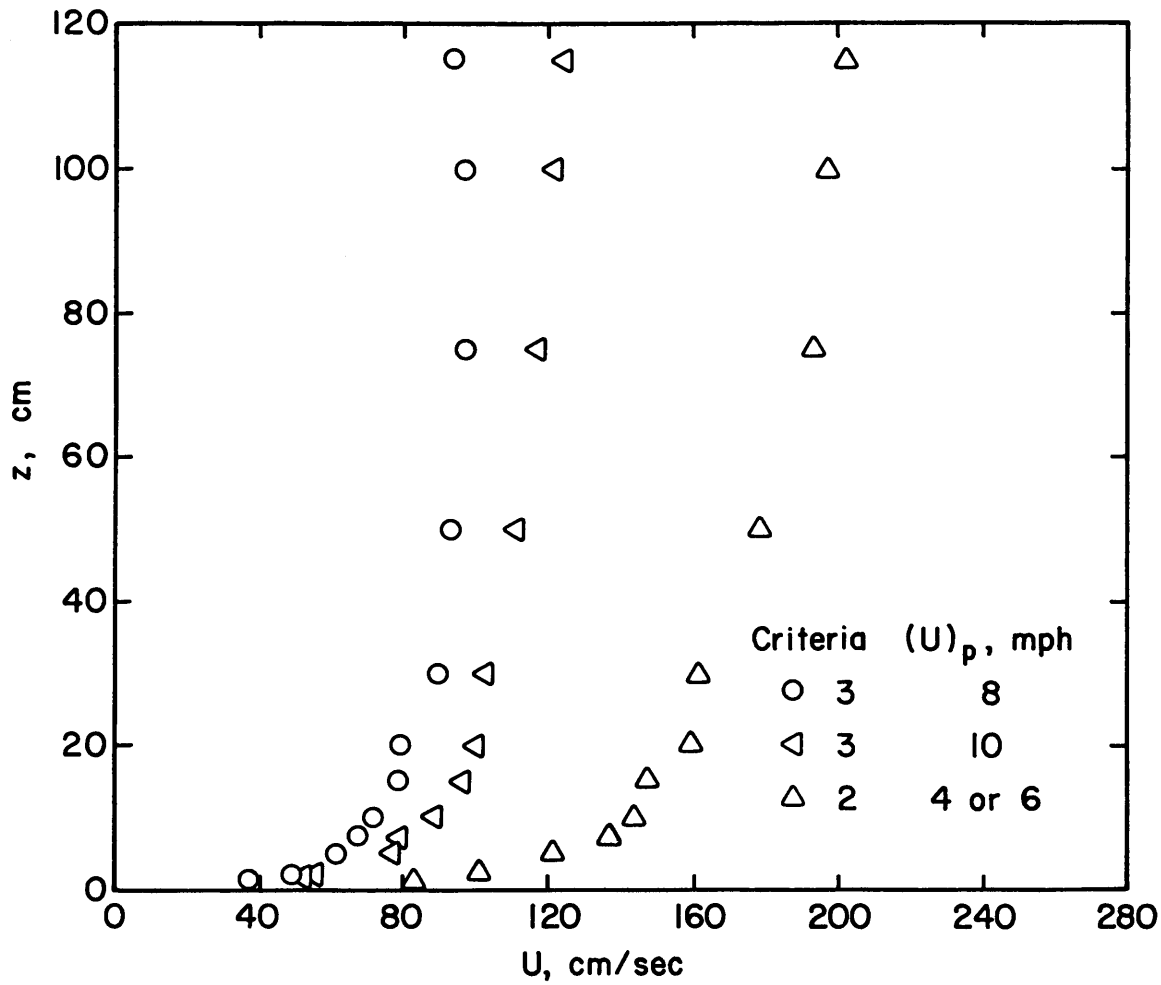

Figure 4b. Velocity Profiles

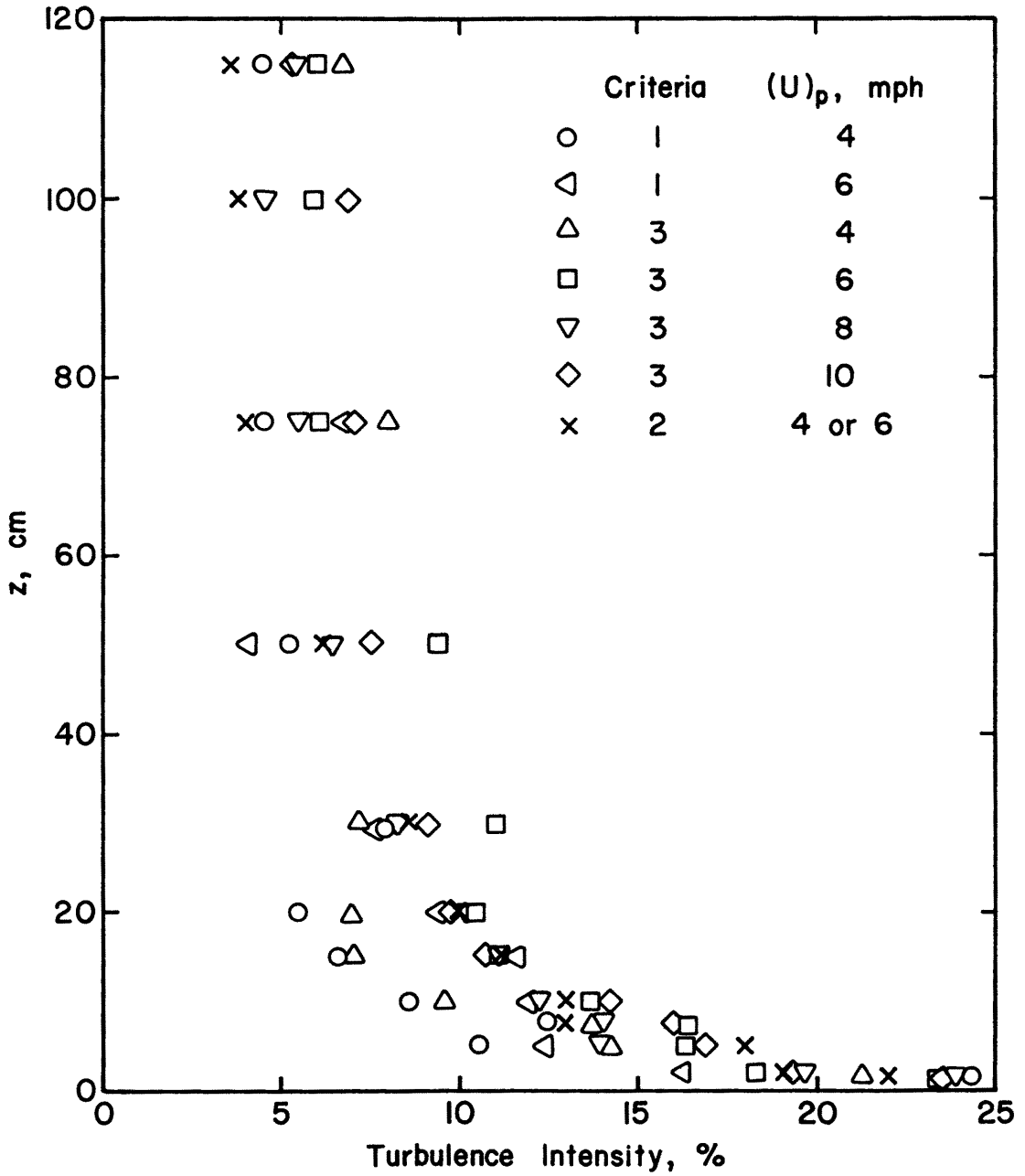

Figure 5. Local Longitudinal Turbulent Intensity Profiles

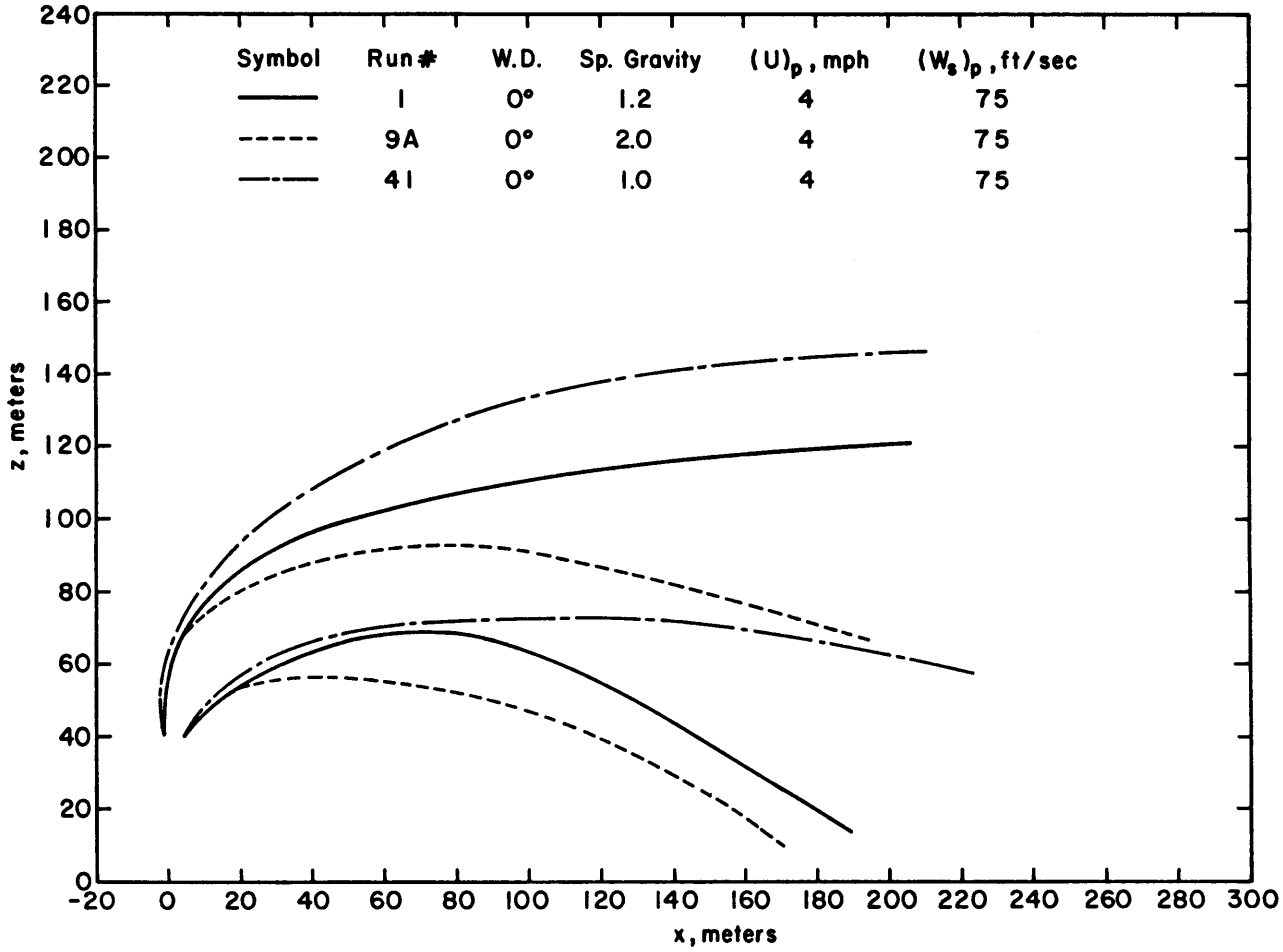

Figure 6. NTF Exhaust Plume Envelopes, $\theta = 0°$, U = 4 mph, W_s = 75 ft/sec, S.G. = 1.2, 1.0 and 2.0

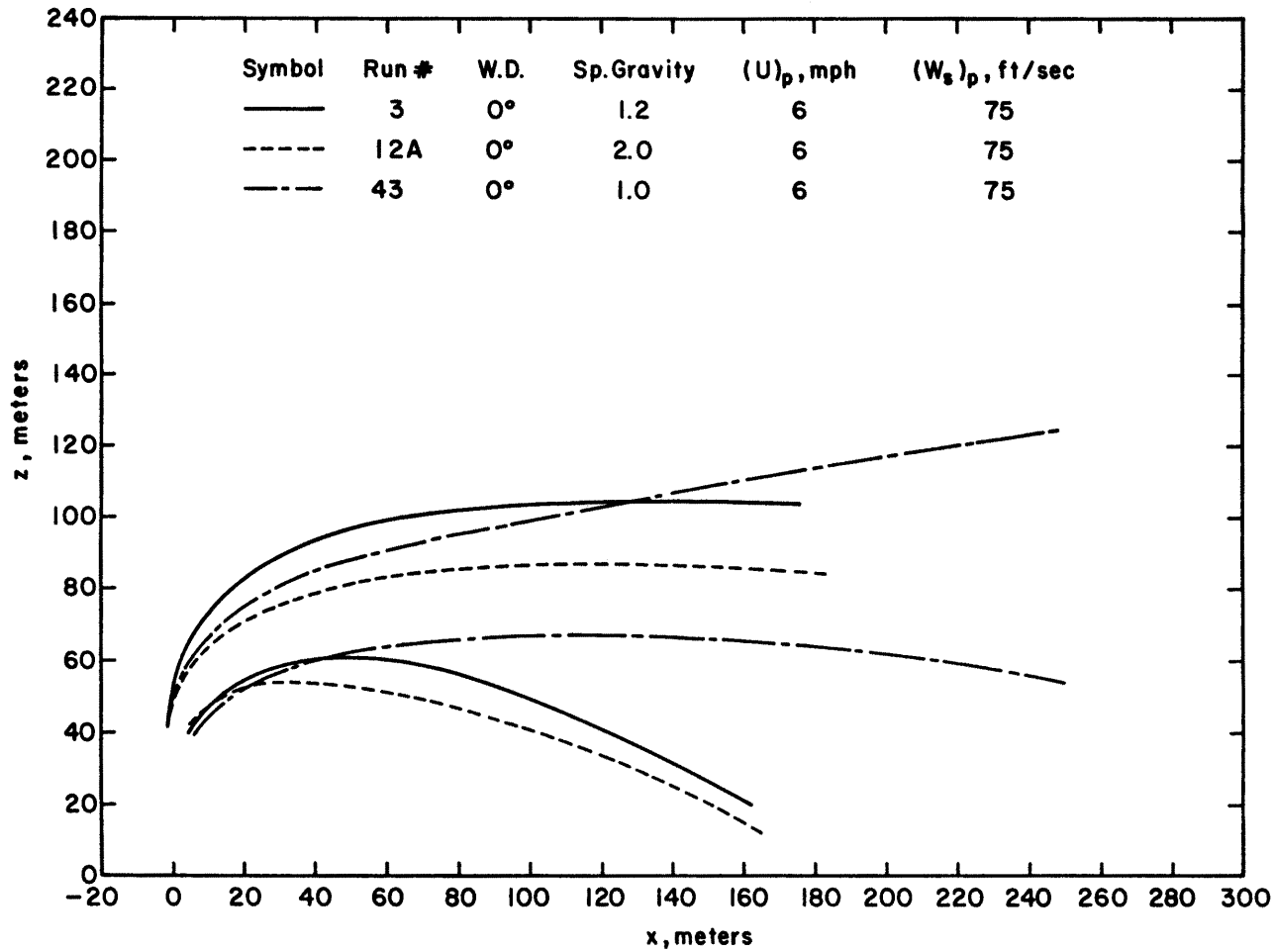

Figure 7a. NTF Exhaust Plume Envelopes, $\theta = 0°$, U = 6 mph, W_s = 75 ft/sec, S.G. = 1.2, 1.0 and 2.0

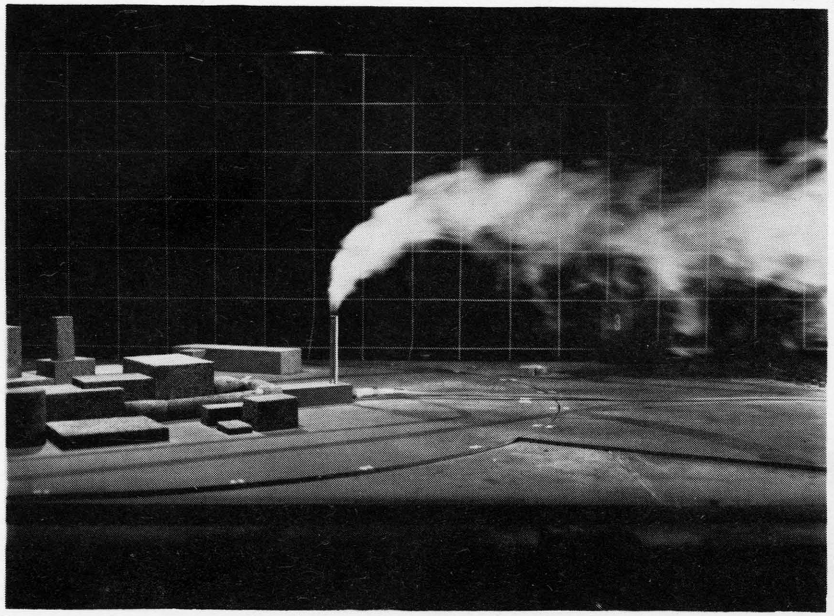

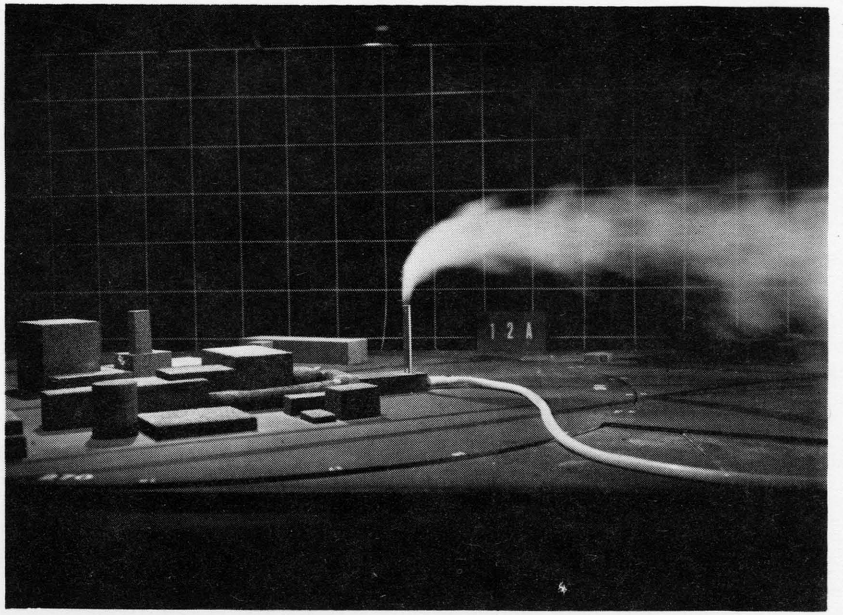

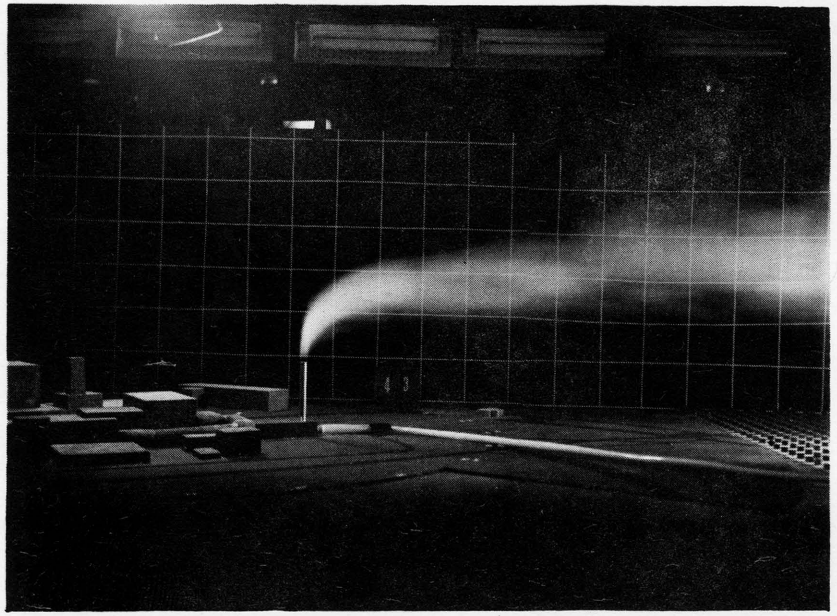

Figure 7b. NTF Exhaust Plume Photographs, $\theta = 0°$, U = 6 mph, W_s = 75 ft/sec, S.G. = 1.2, 1.0 and 2.0

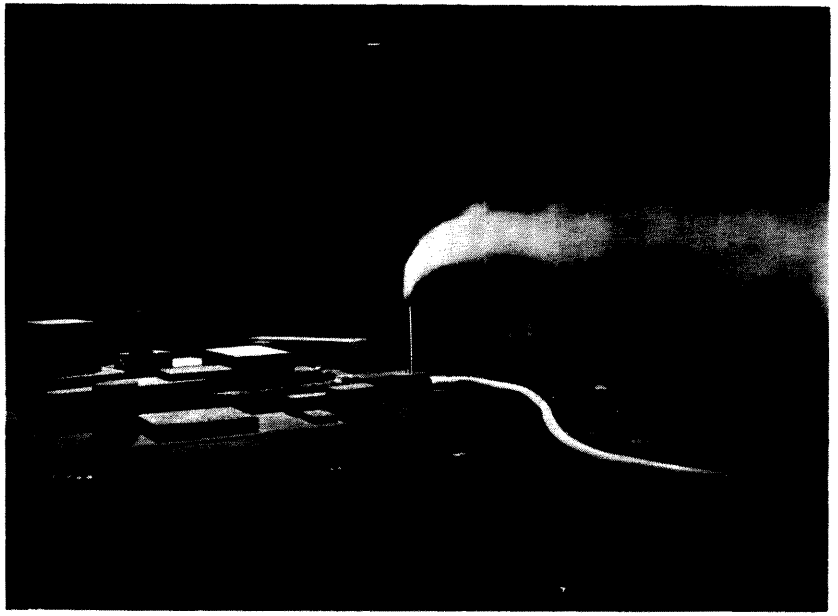

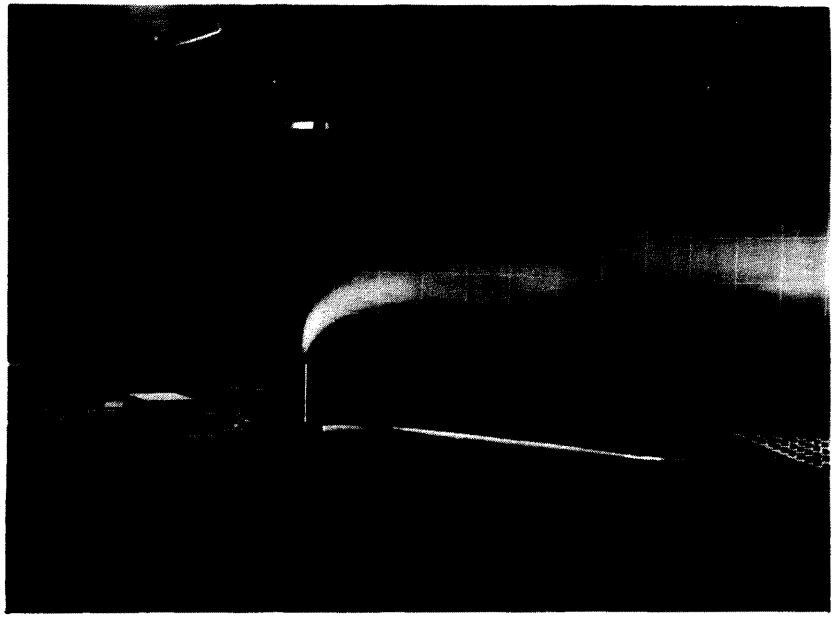

Figure 7b. NTF Exhaust Plume Photographs, $\theta = 0°$, U = 6 mph, W_s = 75 ft/sec, S.G. = 1.2, 1.0 and 2.0

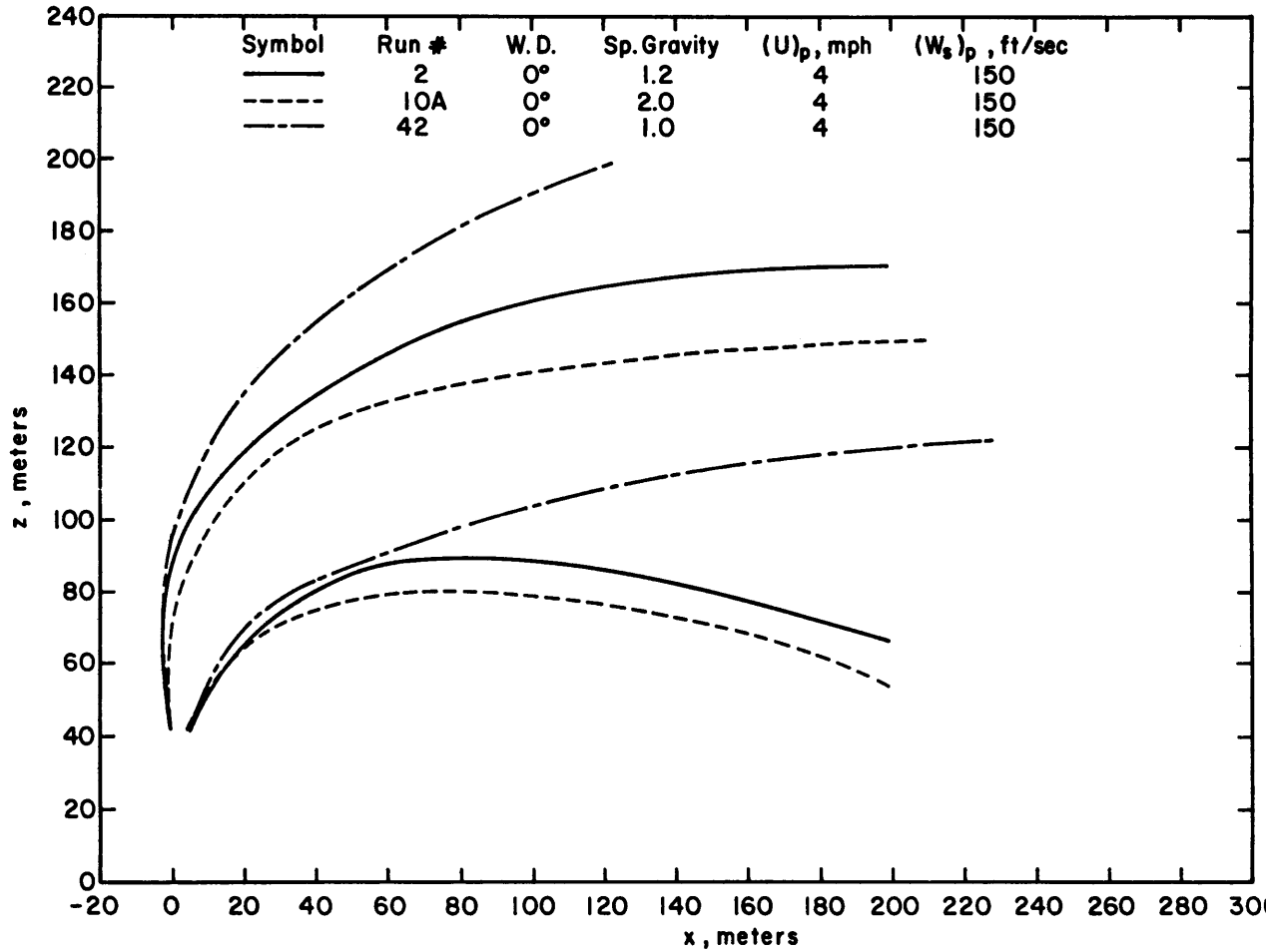

Figure 8. NTF Exhaust Plume Envelopes, $\theta = 0°$, U = 4 mph, W_s = 150 ft/sec, S.G. = 1.2, 1.0 and 2.0

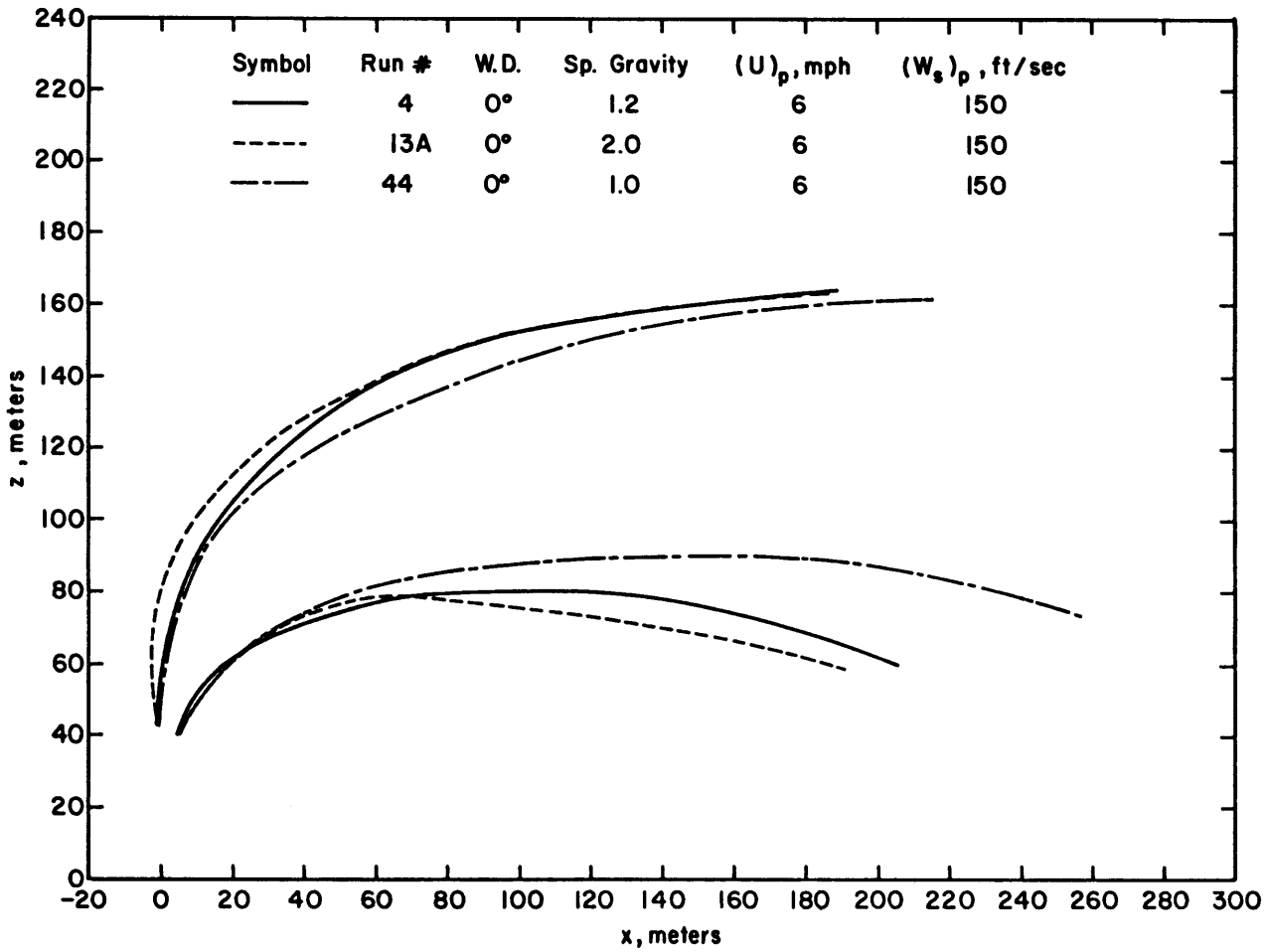

Figure 9a. NTF Exhaust Plume Envelopes, $\theta = 0°$, U = 6 mph, W_s = 150 ft/sec, S.G. = 1.2, 1.0 and 2.0

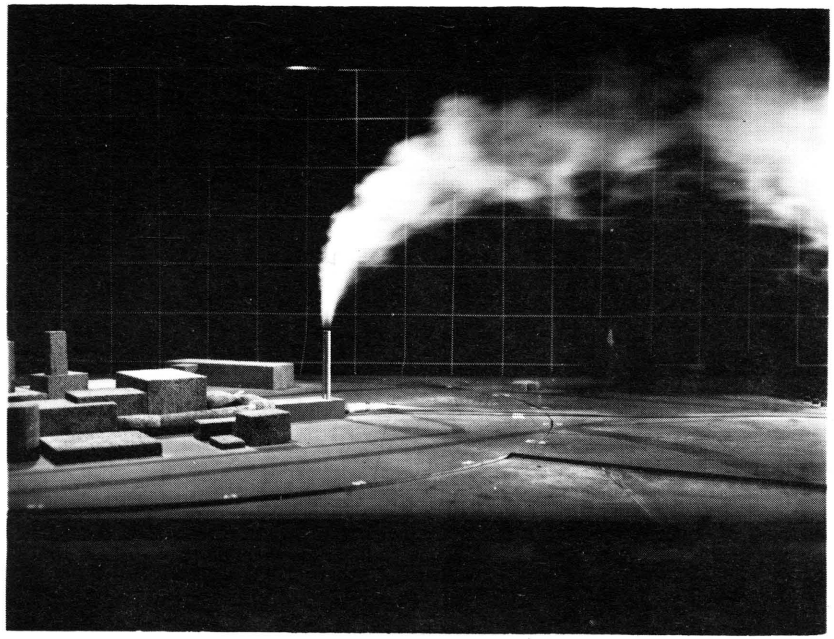

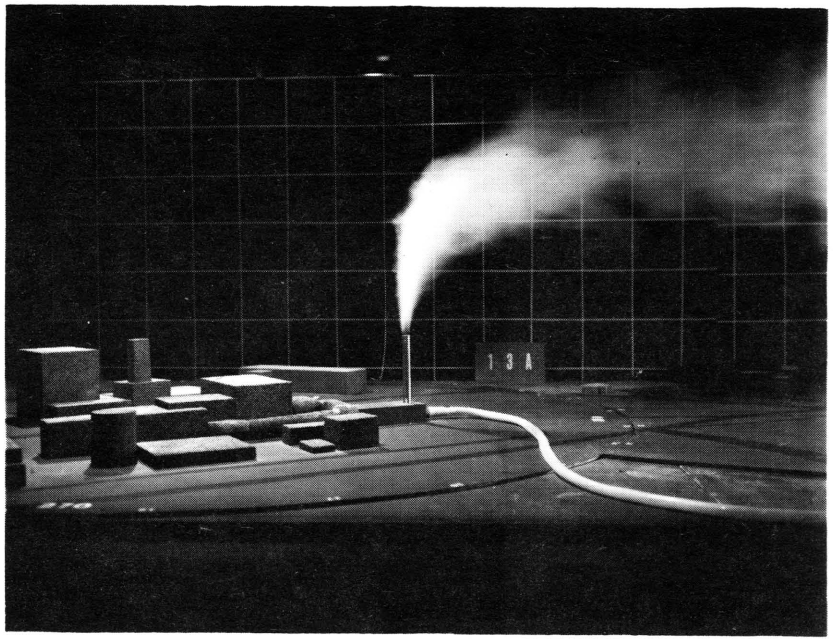

Figure 9b. NTF Exhaust Plume Photographs, $\theta = 0°$, U = 6 mph, W_s = 150 ft/sec, S.G. = 1.2, 1.0 and 2.0

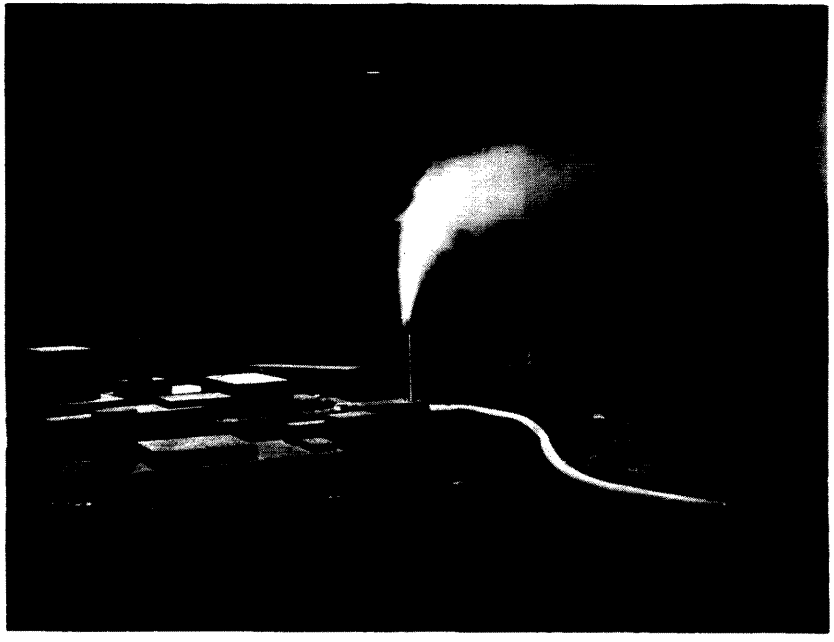

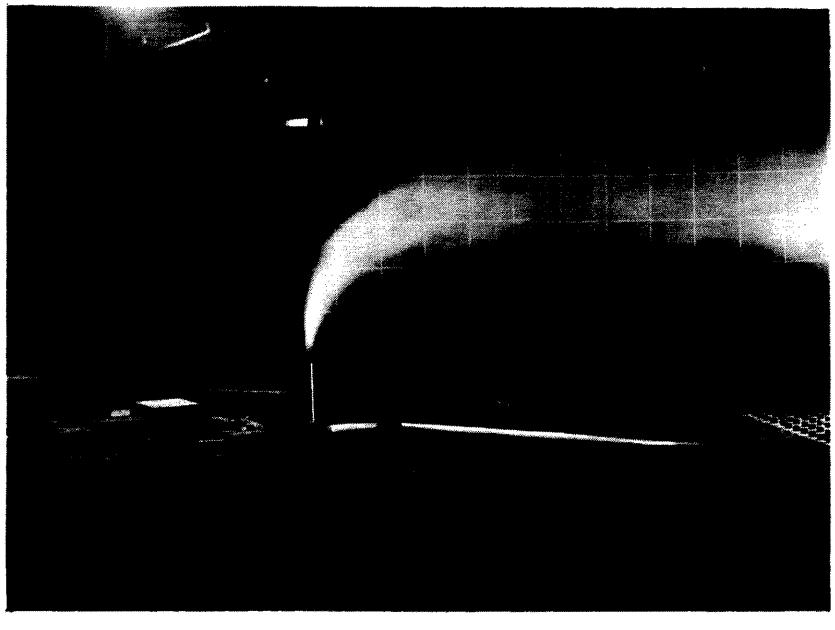

Figure 9b. NTF Exhaust Plume Photographs, $\theta = 0°$, U = 6 mph, W_s = 150 ft/sec, S.G. = 1.2, 1.0 and 2.0

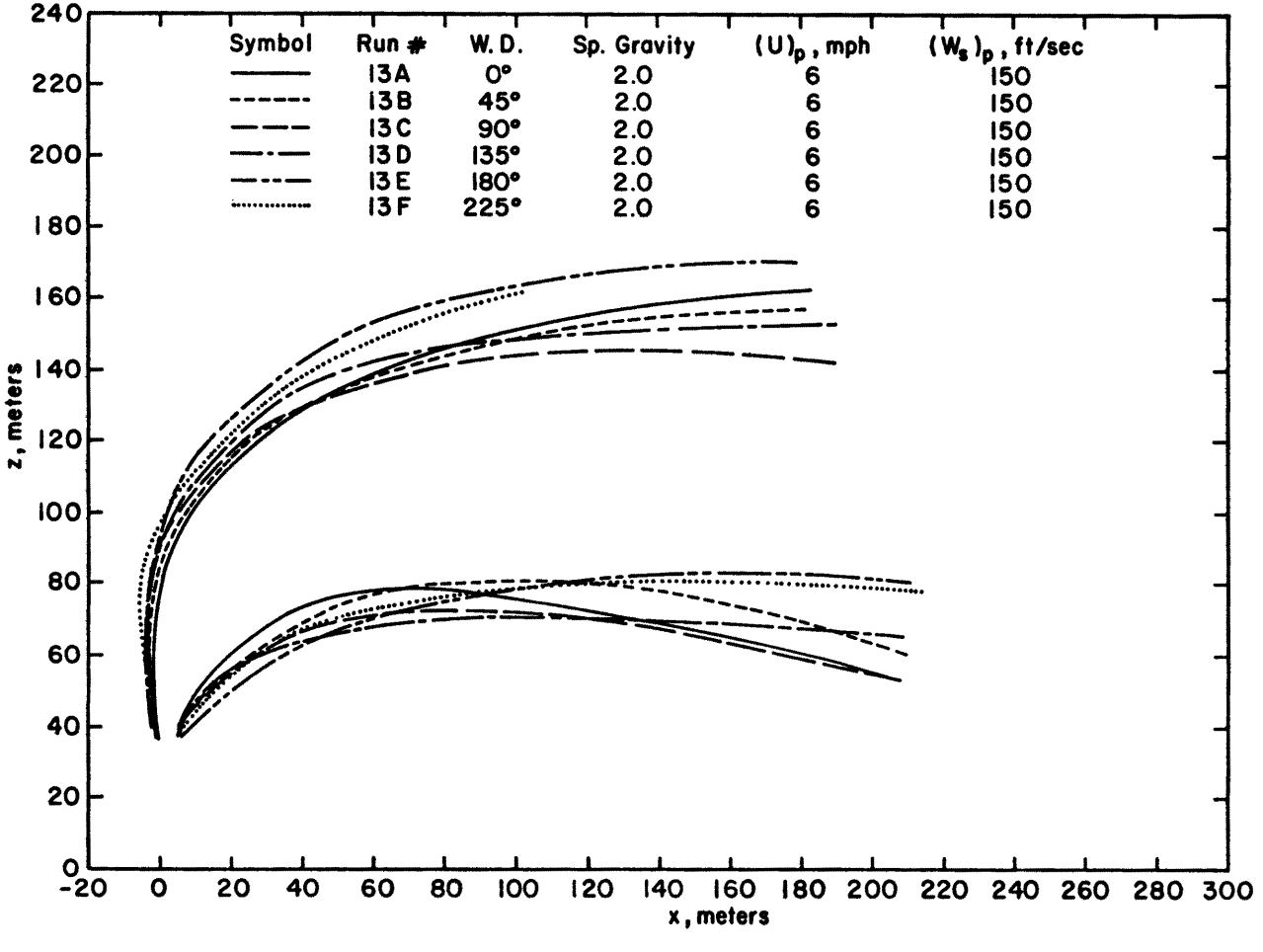

Figure 10a. NTF Exhaust Plume Envelopes, θ = 0 to 225°, U = 6 mph, W_s = 150 ft/sec, S.G. = 2.0

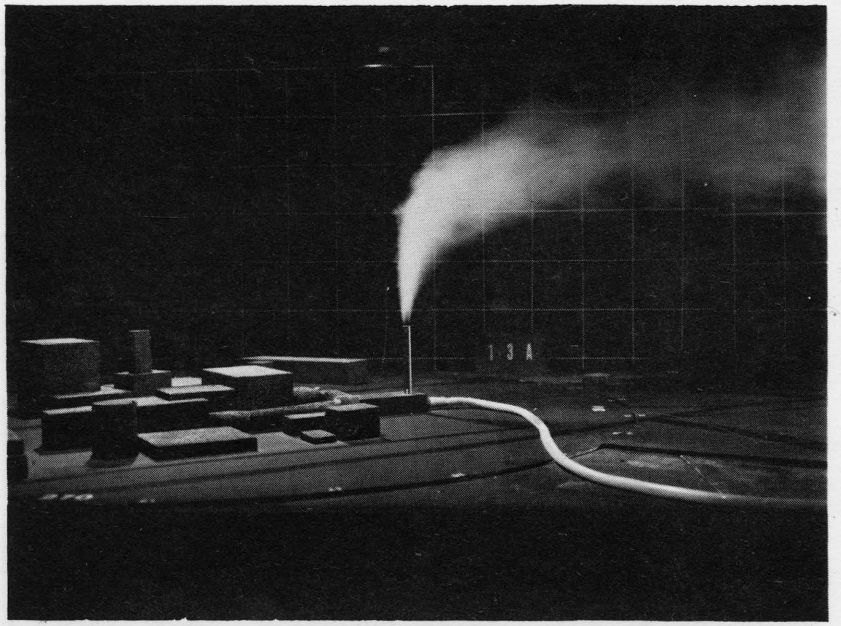

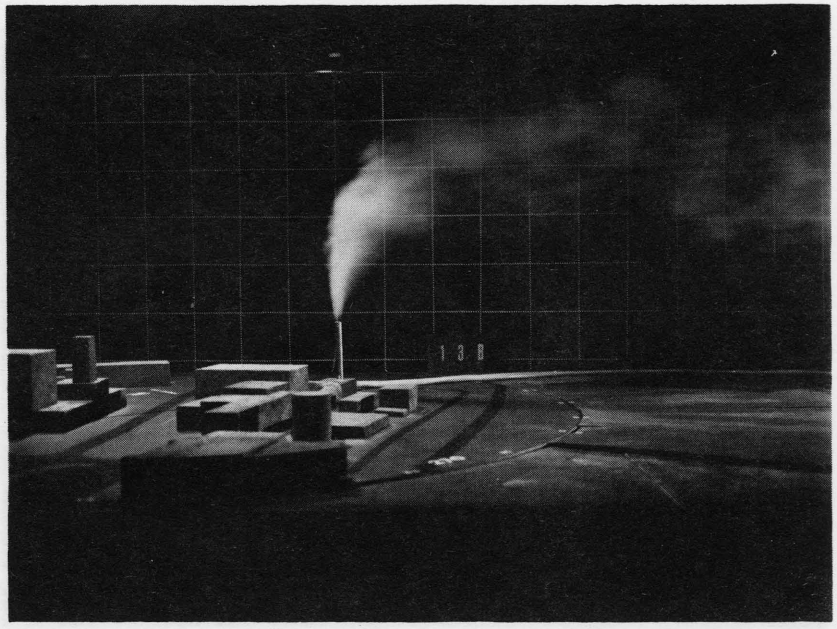

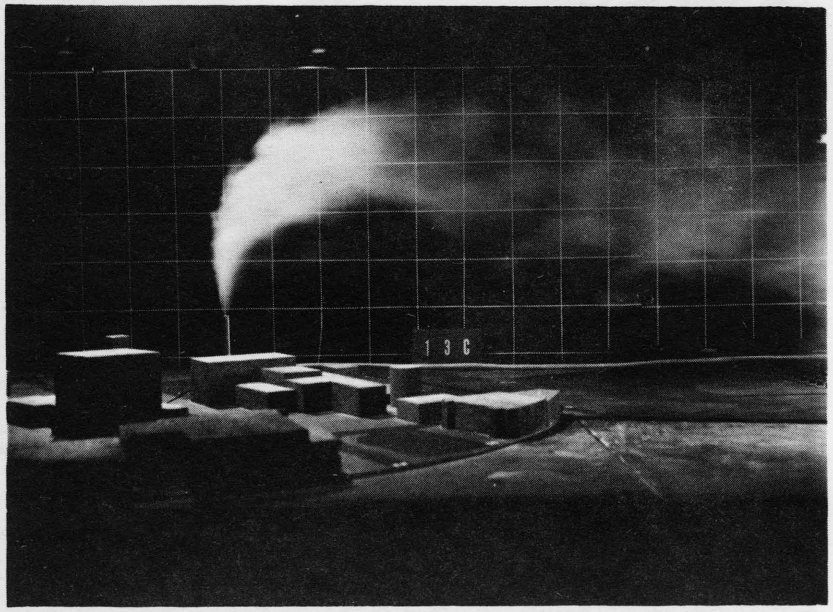

Figure 10b. NTF Exhaust Plume Photographs, θ = 0 to 225°, U = 6 mph, W_s = 150 ft/sec, S.G. = 2.0

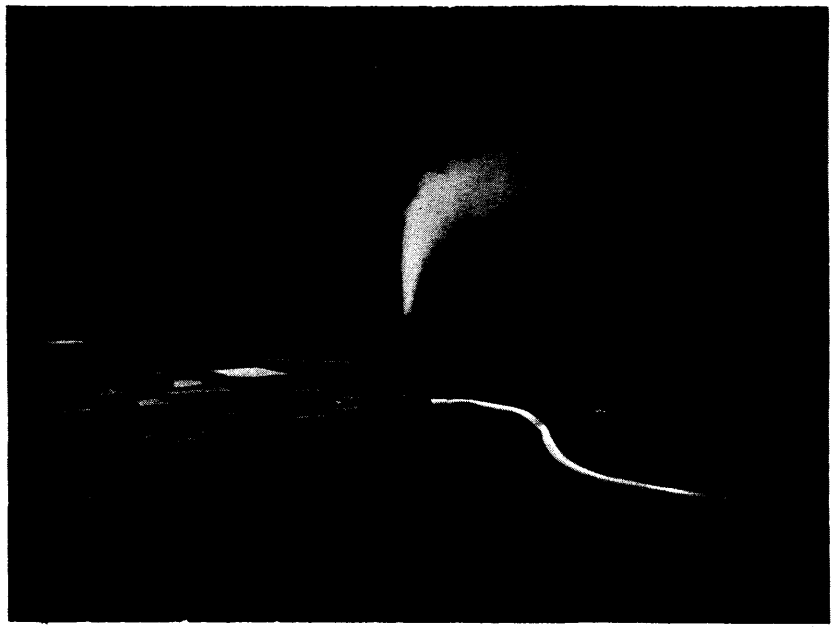

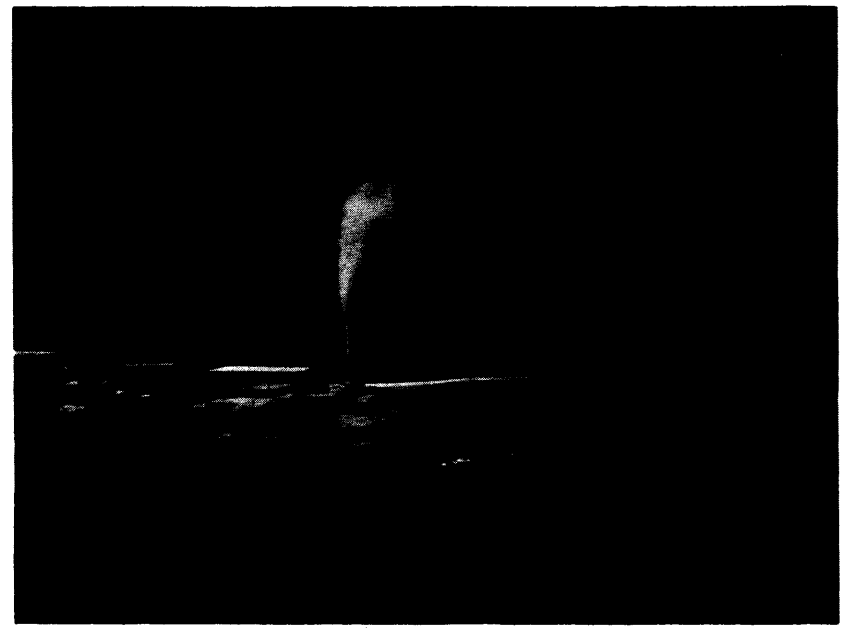

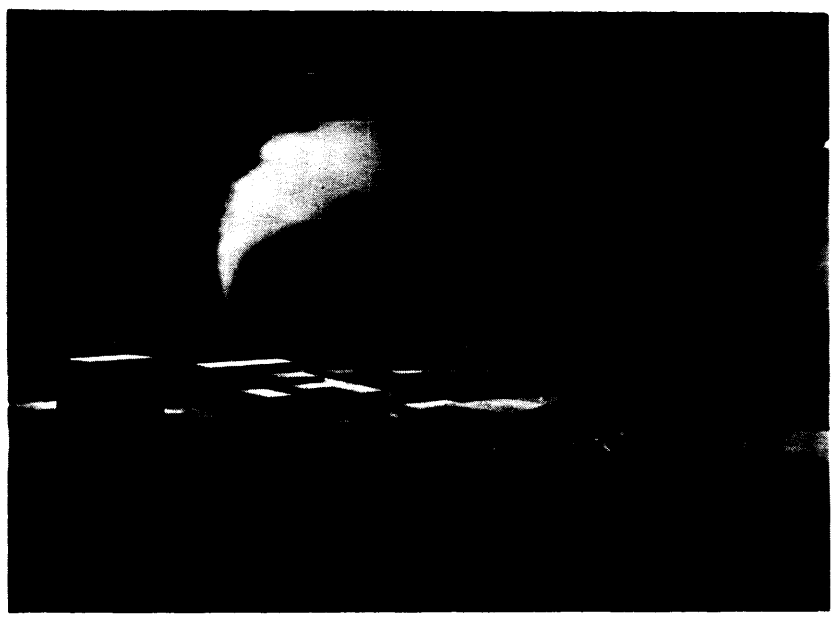

Figure 10b. NTF Exhaust Plume Photographs,
θ = 0 to 225°, U = 6 mph,
W_s = 150 ft/sec, S.G. = 2.0

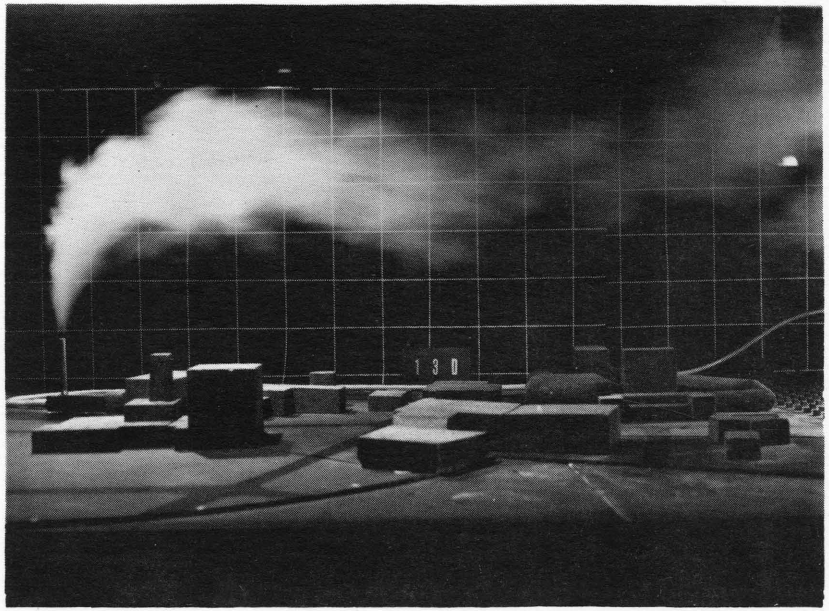

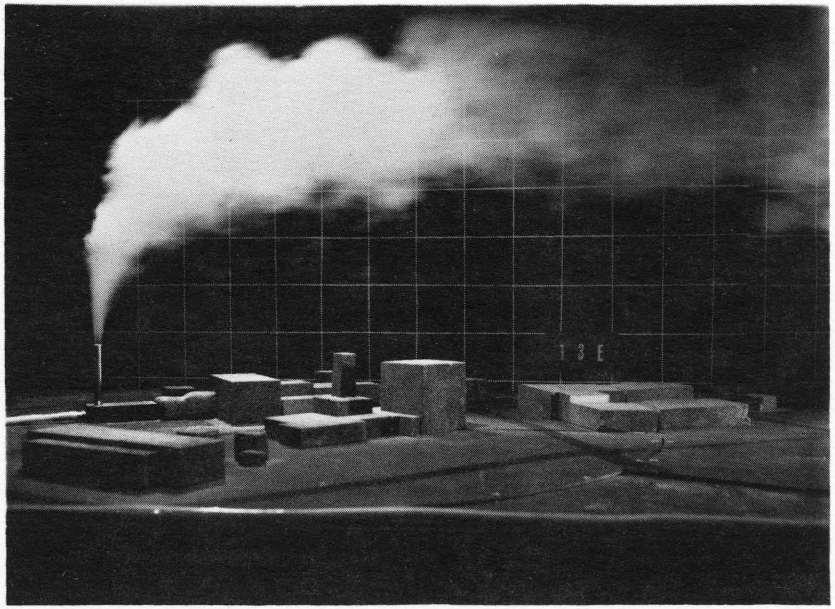

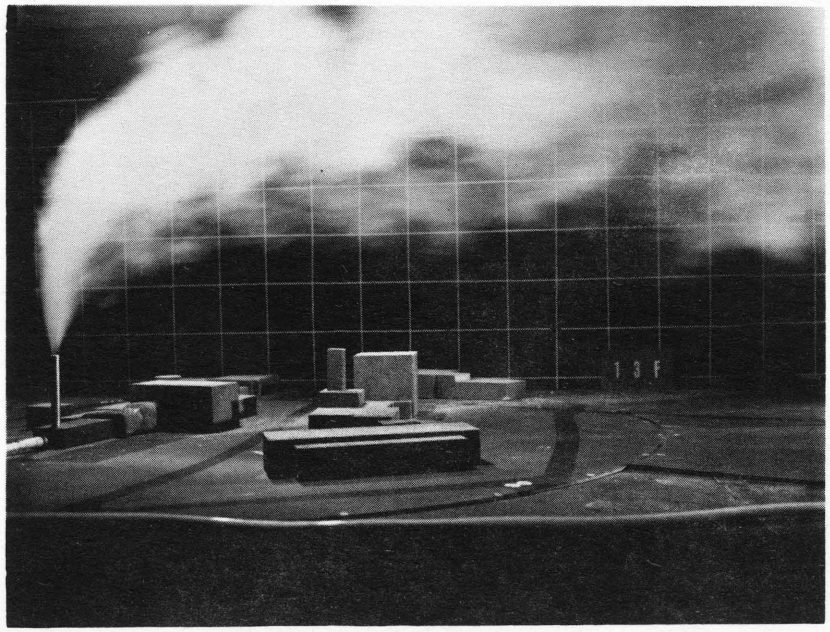

Figure 10c. NTF Exhaust Plume Photographs, θ = 0 to 225°, U = 6 mph, W_s = 150 ft/sec, S.G. = 2.0

Figure 10c. NTF Exhaust Plume Photographs, θ = 0 to 225°, U = 6 mph, W_s = 150 ft/sec, S.G. = 2.0

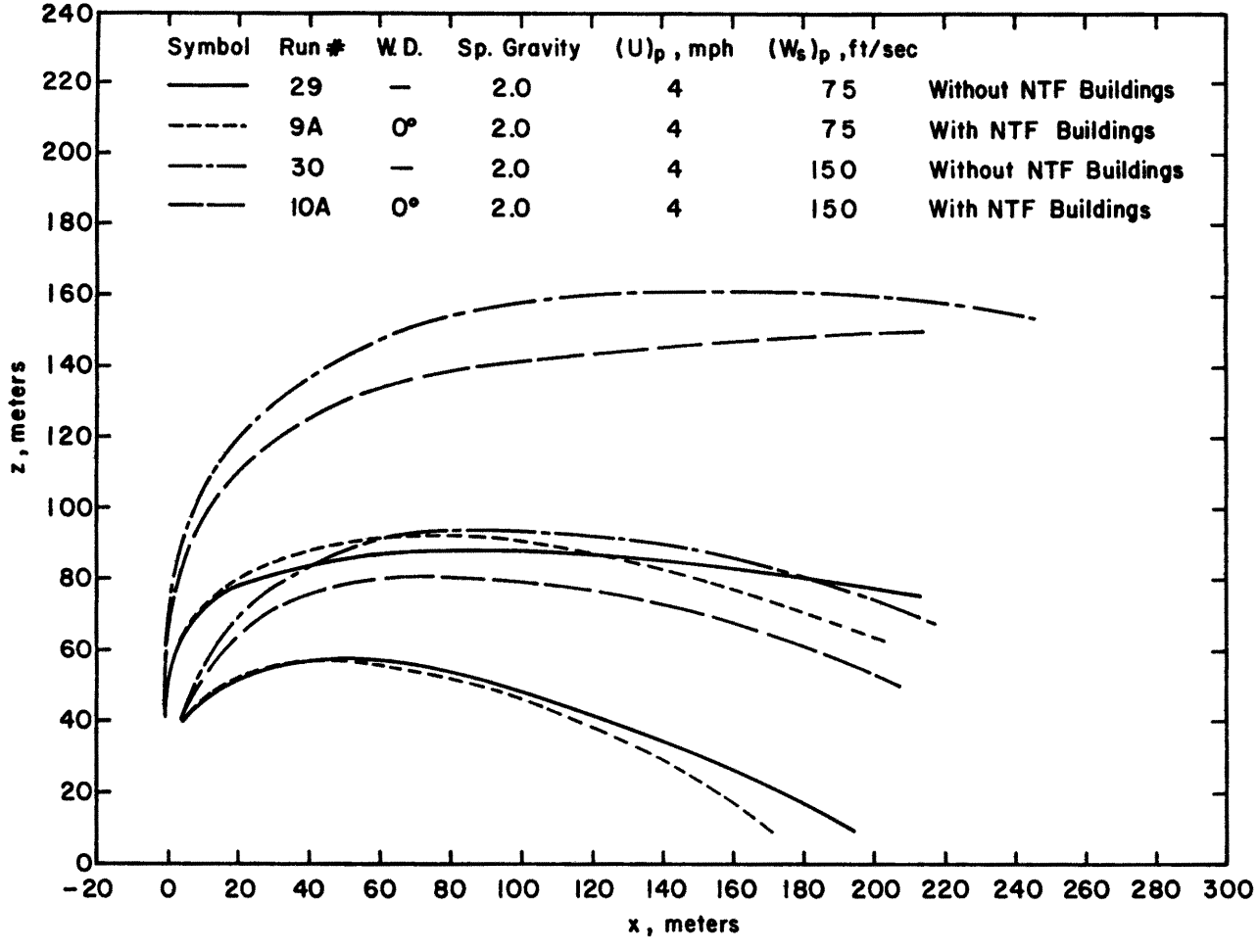

Figure 11a. NTF Exhaust Plume Envelopes, $\theta = 0°$, U = 4 mph, W_s = 75 and 150 ft/sec, S.G. = 2.0 With and Without Model Complex

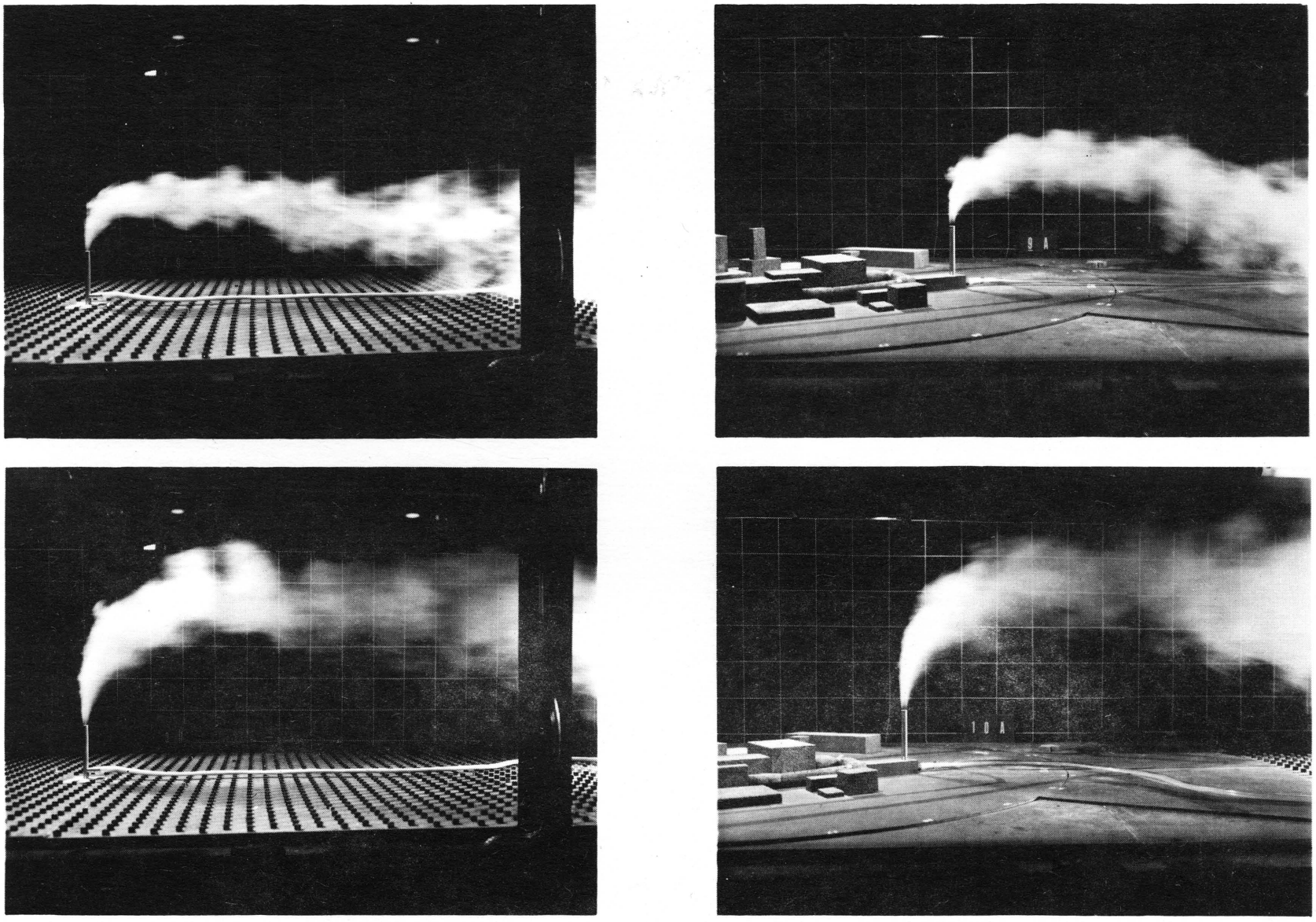

Figure 11b. NTF Exhaust Plume Photographs, θ = 0°, U = 4 mph, W_s = 75 and 150 ft/sec, S.G. = 2.0 with and without Model Complex

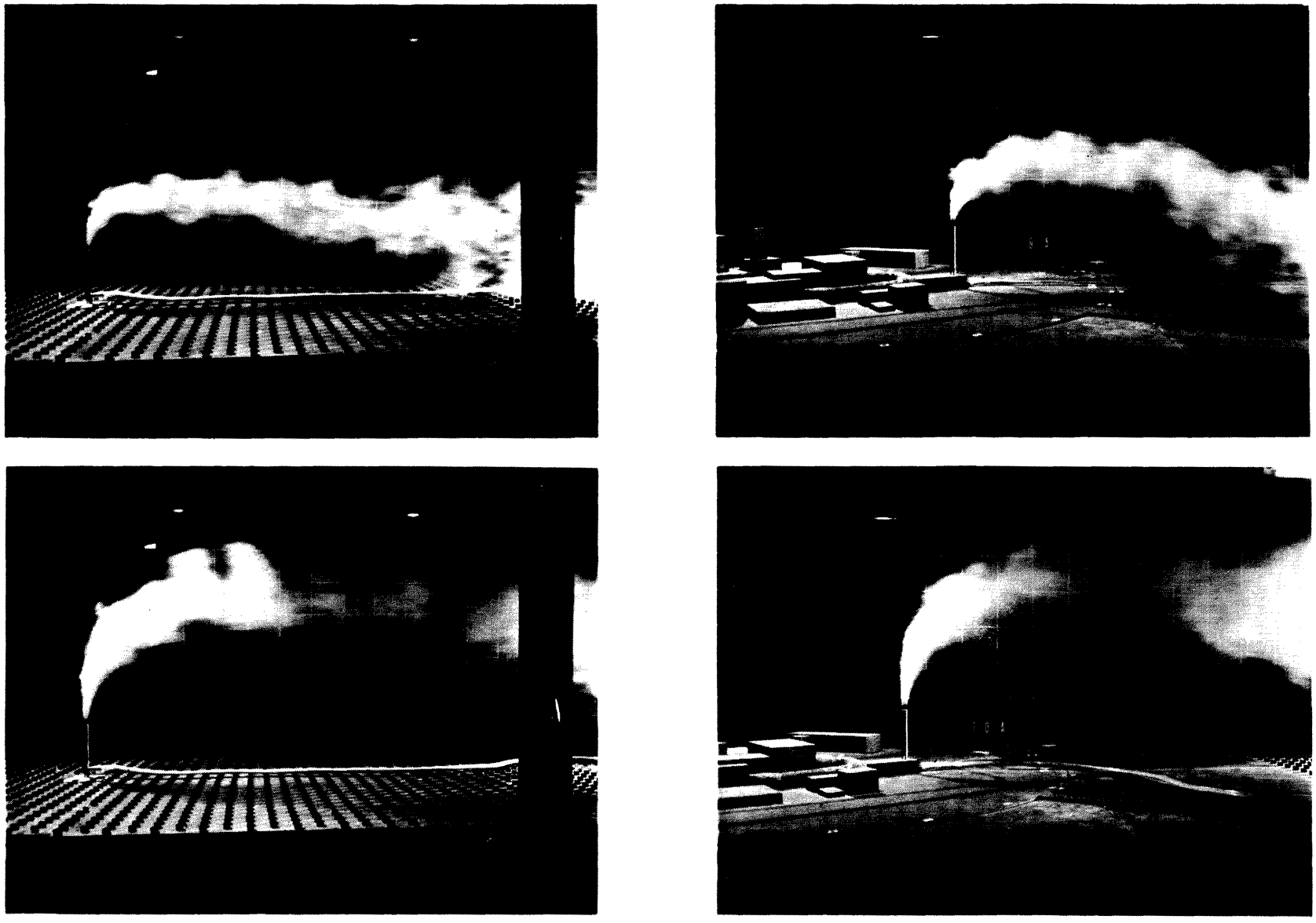

Figure 11b. NTF Exhaust Plume Photographs, $\theta = 0°$, U = 4 mph, W_s = 75 and 150 ft/sec, S.G. = 2.0 with and without Model Complex

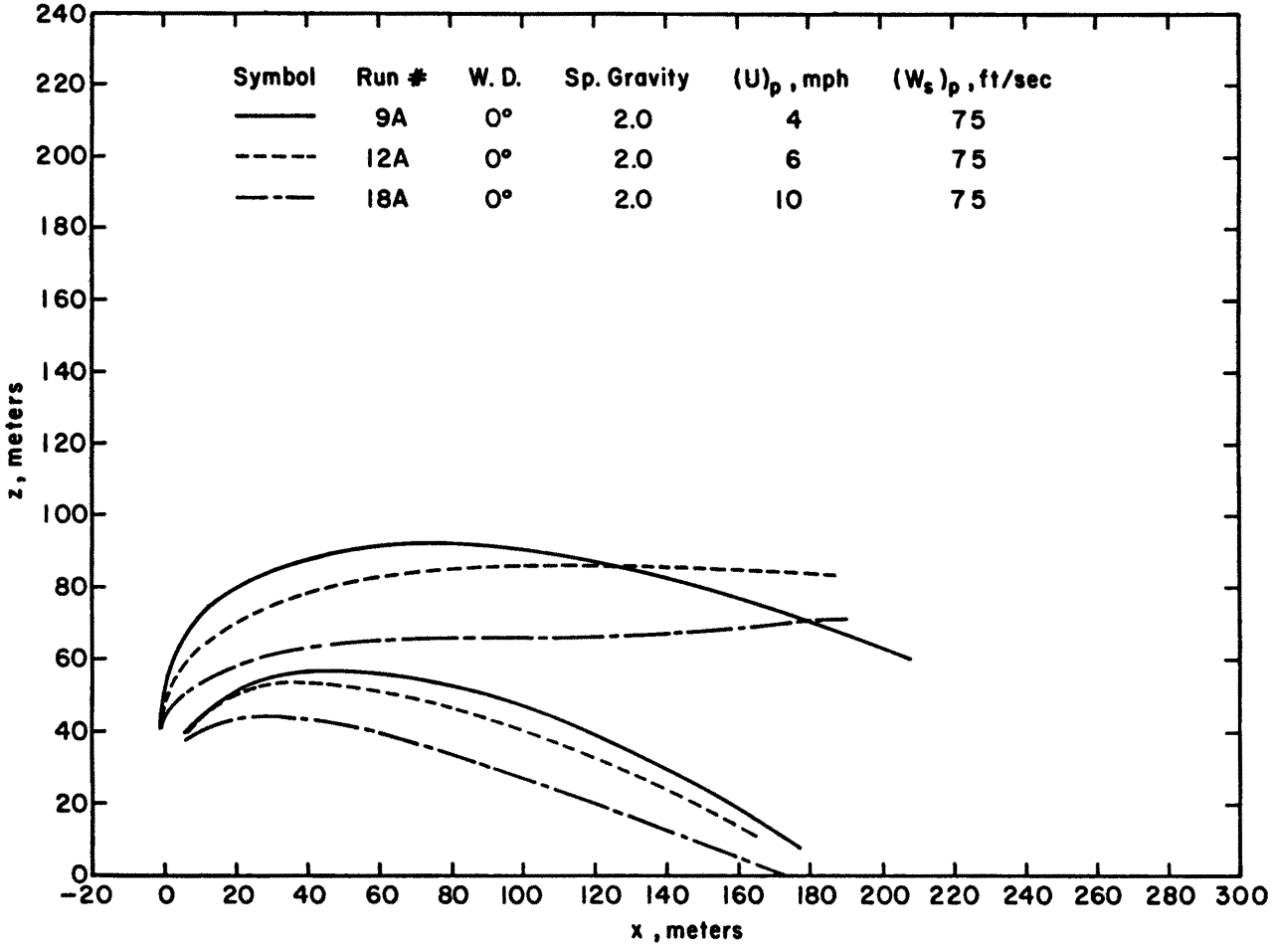

Figure 12a. NTF Exhaust Plume Envelopes, $\theta = 0°$, U = 4, 6 and 10 mph, W_s = 75 ft/sec, S.G. = 2.0

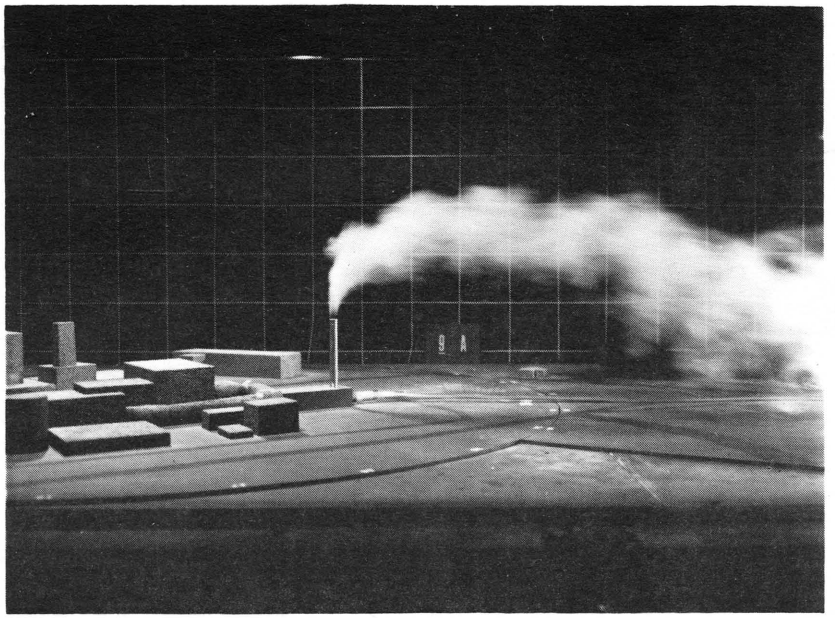

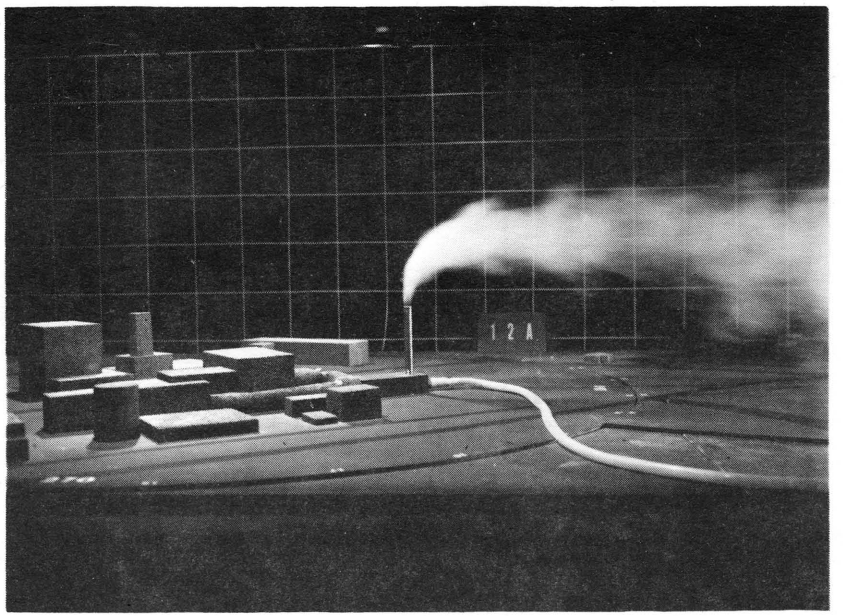

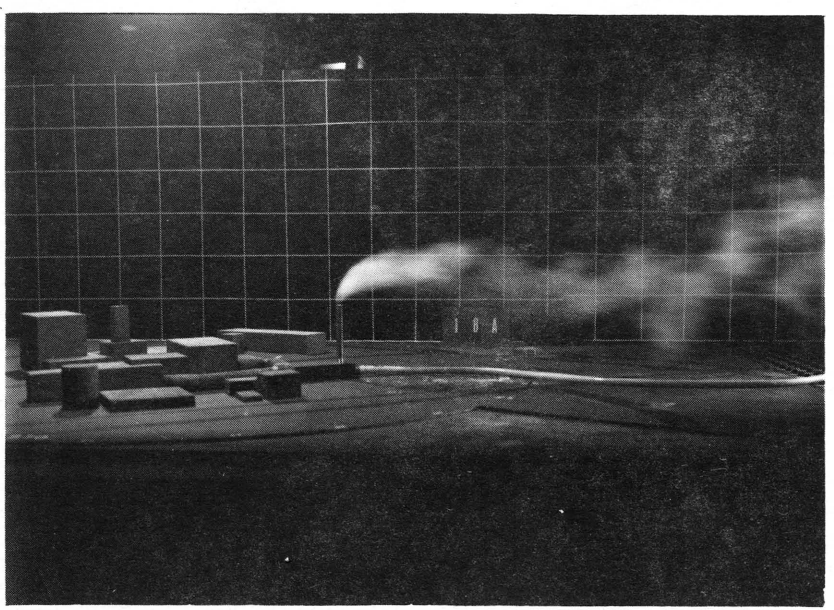

Figure 12b. NTF Exhaust Plume Photographs, $\theta = 0°$, U = 4, 6 and 10 mph, W_s = 75 ft/sec, S.G. = 2.0

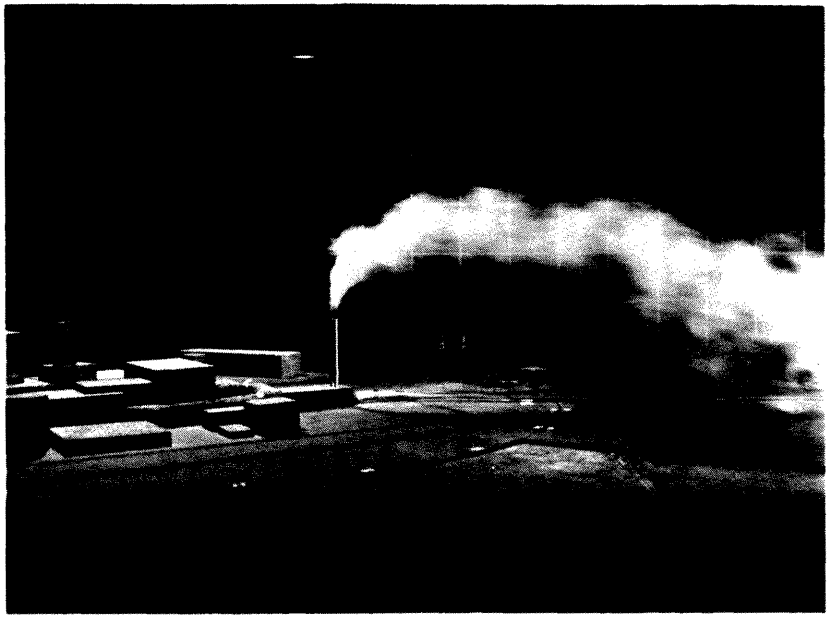

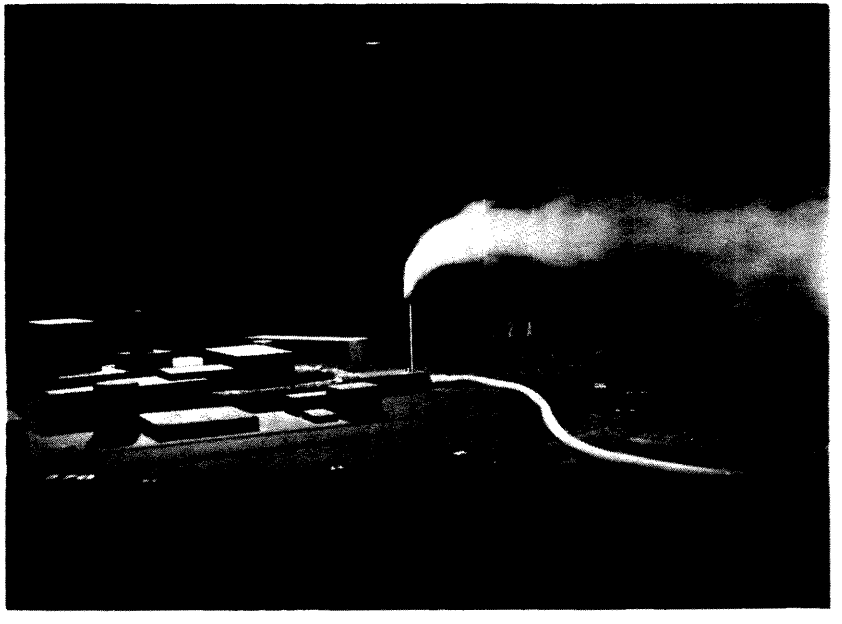

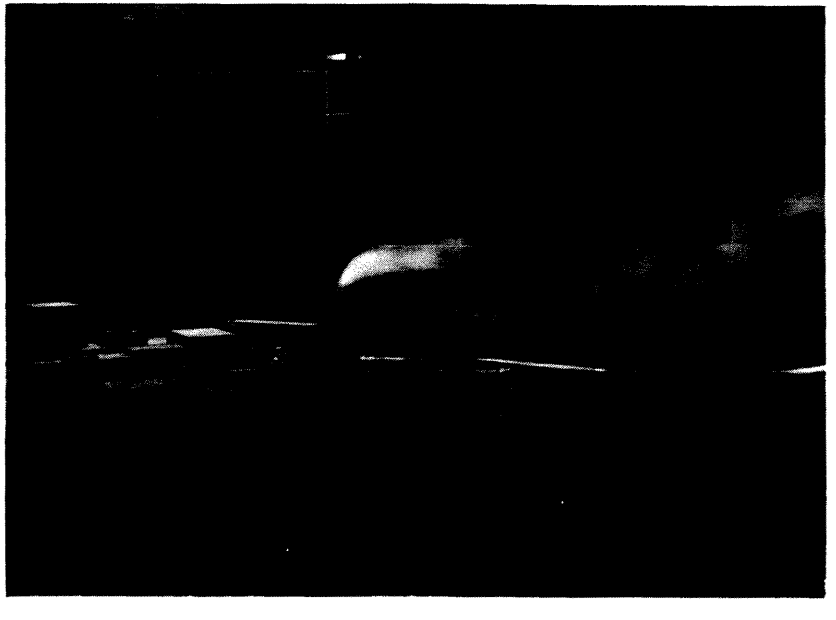

Figure 12b. NTF Exhaust Plume Photographs, $\theta = 0°$, U = 4, 6 and 10 mph, W_s = 75 ft/sec, S.G. = 2.0

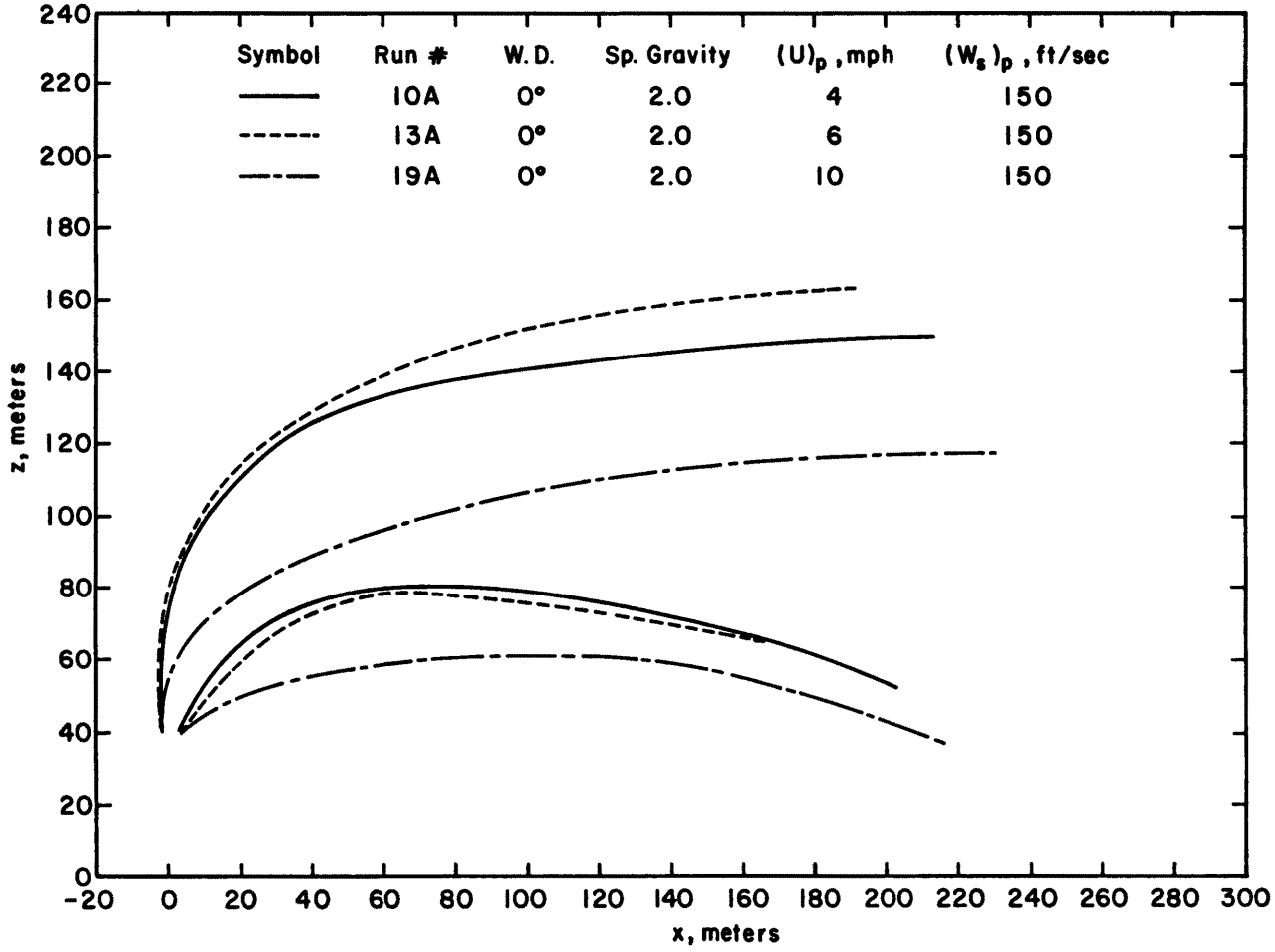

Figure 13a. NTF Exhaust Plume Envelopes, $\theta = 0°$, U = 4, 6 and 10 mph, W_s = 150 ft/sec, S.G. = 2.0

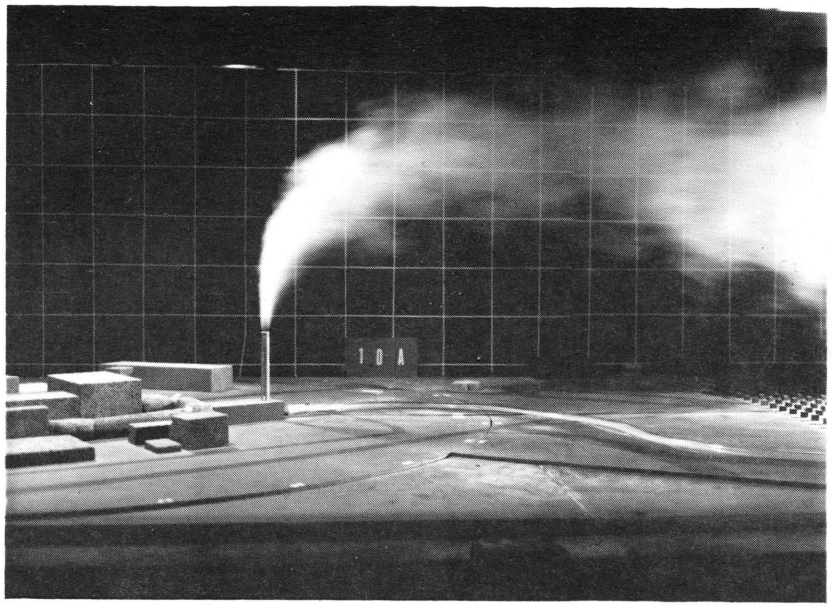

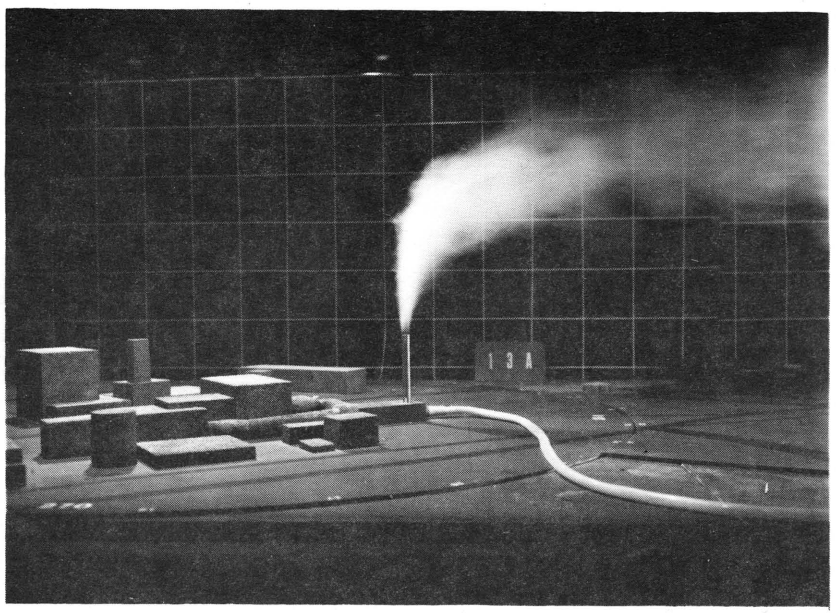

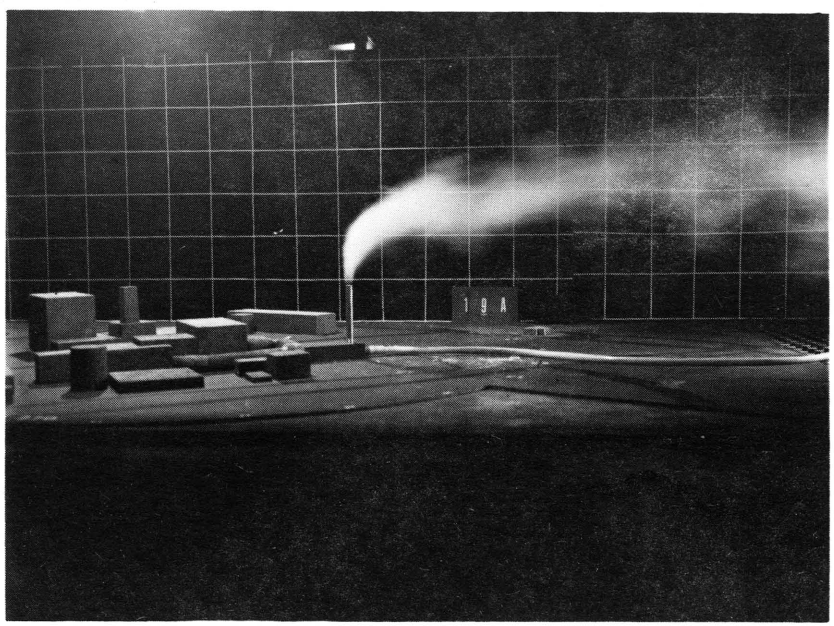

Figure 13b. NTF Exhaust Plume Photographs, $\theta = 0°$, U = 4, 6 and 10 mph, W_s = 150 ft/sec, S.G. = 2.0

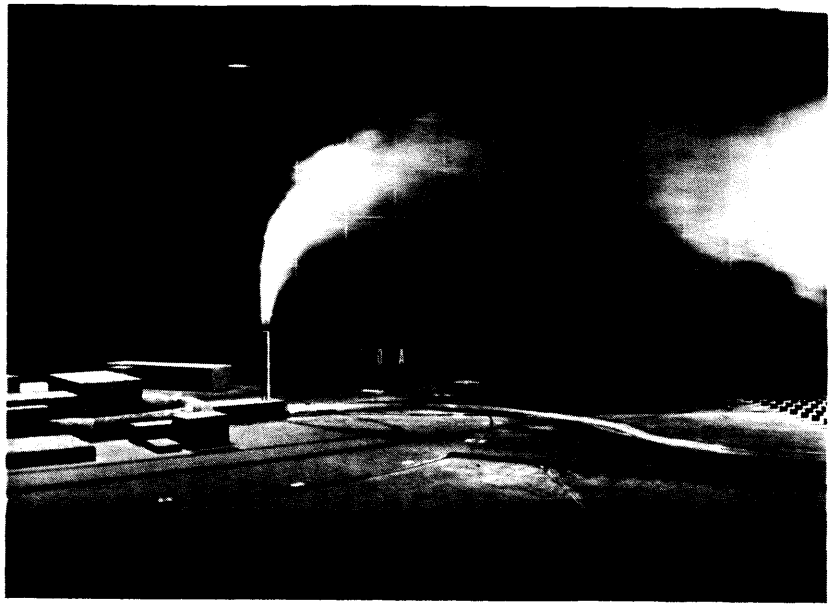

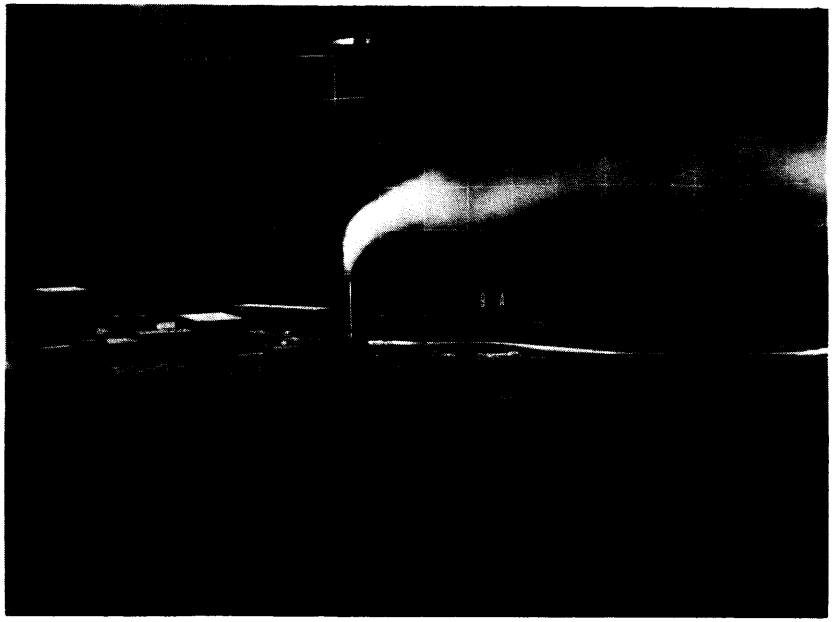

Figure 13b. NTF Exhaust Plume Photographs, $\theta = 0°$, U = 4, 6 and 10 mph, W_s = 150 ft/sec, S.G. = 2.0

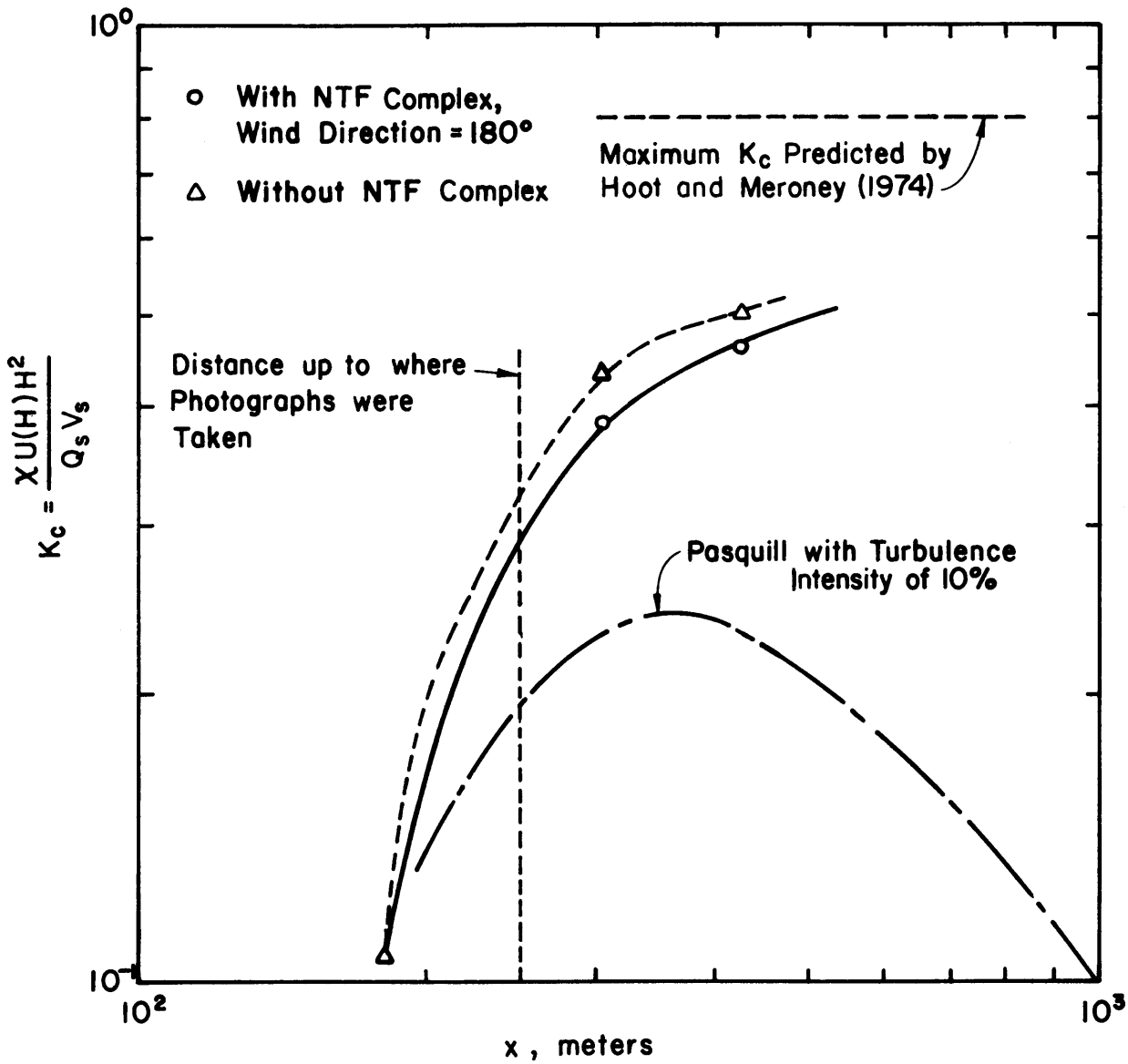

Figure 14. Ground Level Concentration Results